It is also important to note that the fetal spinal cord NSC-derived neurons extended their neurites well (visualized by Tα1-EYFP expression) within the host spinal cord, even in the presence of CNS myelin, which should include inhibitors against axonal extension and regeneration. Recently, Dr. Marie Filbin and her colleagues showed that an elevation of cAMP in neurons can overcome the inhibition of axonal growth by MAG and CNS myelin [50]. The elevation of cAMP results in the synthesis of polyamines, due to an up-regulation of Arginase I, a key enzyme in their synthesis. Interestingly, endogenous Arginase I levels are high in young dorsal root ganglia (DRG) neurons but drop spontaneously when the DRGs reach an age that coincides with the switch from promotion to inhibition by MAG/myelin, which might correspond to our above-mentioned behaviors of neuronal axons derived from grafted fetal spinal cord NSCs.

2. Conclusions and perspectives

We have shown that in vitro-expanded NSCs can contribute to the repair of the injured spinal cord in a rat model, when they are transplanted at the appropriate time point. The differentiation of transplanted neural progenitor cells, including NSCs, into neurons and oligodendrocytes, which may correspond to the behavioral recovery we observed, depends on the microenvironment [25]. To achieve more efficient therapeutic strategies, it is likely that the concomitant use of NSC transplantation, blockade of CNS myelin-derived inhibitors against axonal regeneration, and administration of neurotrophic factors [51,52] would improve the method. To apply these basic experimental results to clinical practice in the near future, it is urgent to establish a pre-clinical experimental system using primates, which are closer to humans, and we are currently addressing this problem. It is also indispensable to establish a system to produce and supply large-scale human NSCs for clinical use. We are working towards achieving this challenging goal in a tight collaboration with Drs. Jun Miyake, Yonehiro Kanemura, and their colleagues of the Tissue Engineering Research Center (TERC), at the National Institute of Advanced Industrial Science and Technology (AIST) in Japan. We recently established a relatively large-scale culture of human NSCs [19], but the conditions need to be improved to maintain the safety and stability of these cells in large cultures before they can be used in future therapeutic applications. Furthermore, it is obviously important to approach the application to humans step-by-step, linking animal experiments with studies using progressively modified technology in small number of patients, using well validated assessment protocols [53]. We have no doubt that once these challenging problems are resolved, the day will surely come when regenerative therapy with NSCs for spinal cord injuries will be possible.

Acknowledgements

We thank Dr. Barbara Bregman for her invaluable discussions and suggestions and Kumiko Inoue and Akiyo Hirayama for their help in preparing the manuscript and excellent administrative assistance. Work in the author's laboratory was supported by grants from the Japanese Ministry of Education, Culture, Sports, Science and Technology, and from the Japan Science and Technology Corporation (CREST).

References

[1] Ramon y Cajal S. Degeneration and regeneration of the nervous system. Oxford: Oxford University Press; 1928 [Day RM, Trans.; from the 1913 Spanish ed.].
[2] Johansson CB, Momma S, Clarke DL, Risling M, Lendahl U, Frisen J. Identification of a neural stem cell in the adult mammalian central nervous system. Cell 1999;96:25–34.
[3] Widenfalk J, Lundstromer K, Jubran M, Brene S, Olson L. Neurotrophic factors and receptors in the immature and adult spinal cord after mechanical injury or kainic acid. J Neurosci 2001;21:3457–75.
[4] Richardson PM, McGuinness UM, Aguayo AJ. Axons from CNS neurons regenerate into PNS grafts. Nature 1980;284:264–5.
[5] Bregman BS. Spinal cord transplants permit the growth of serotonergic axons across the site of neonatal spinal cord transection. Dev Brain Res 1987;34:265–79.
[6] Cai D, Shen Y, De Bellard M, Tang S, Filbin MT. Prior exposure to neurotrophins blocks inhibition of axonal regeneration by MAG and myelin via a cAMP-dependent mechanism. Neuron 1999;22:89–101.
[7] Chen MS, Huber AB, van der Haar ME, Frank M, Schnell L, Spillmann AA, et al. Nogo-A is a myelin-associated neurite outgrowth inhibitor and an antigen for monoclonal antibody IN-1. Nature 2000;403:434–9.
[8] Miya D, Giszter S, Mori F, Adipudi V, Tessler A, Murray M. Fetal transplants after the development of function after spinal cord transection in newborn rats. J Neurosci 1997;17:4856–72.
[9] Diener PS, Bregman BS. Fetal spinal cord transplants support the development of target reaching and coordinated postural adjustments after neonatal cervical spinal cord injury. J Neurosci 1998;18:763–78.
[10] Diener PS, Bregman BS. Fetal spinal cord transplants support growth of supraspinal and segmental projections after cervical spinal cord hemisection in the neonatal rat. J Neurosci 1998;18:779–93.
[11] Freed WJ. Neural transplantation: an introduction. Cambridge, MA: MIT Press; 1999.
[12] Aguayo AJ, David S, Bray GM. Influences of the glial environment on the elongation of axons after injury. Transplantation studies in adult rodents. J Exp Biol 1981;95:231–40.
[13] Piccini P, Brooks DJ, Bjorklund A, Gunn RN, Grasby PM, Rimoldi O, et al. Dopamine release from nigral transplants visualized in vivo in a Parkinson's patient. Nat Neurosci 1999;2:1137–40.
[14] Reynolds BA, Weiss S. Generation of neurons and astrocytes from isolated cells of adult mammalian central nervous system. Science 1992;255:1707–10.
[15] Magavi SS, Leavitt BR, Macklis JD. Induction of neurogenesis in the neocortex of adult mice. Nature 2000;405:951–5.
[16] Nakatomi H, Kuriu T, Okabe S, Yamamoto S, Hatano O, Kawahara N, et al. Regeneration of hippocampal pyramidal neurons after ischemic brain injury by recruitment of endogenous neural progenitors. Cell 2002;110:429–41.
[17] Arvidsson A, Collin T, Kirik D, Kokaia Z, Lindvall O. Neuronal replacement from endogenous precursors in the adult brain after stroke. Nat Med 2002;8:963–70.

[18] Svendsen CN, ter Borg MG, Armstrong RJE, Rosser AE, Chandran S, Ostenfeld T, et al. A new method for the rapid and long-term growth of human neural precursor cells. J Neurosci Methods 1998;85:141–52.
[19] Kanemura Y, Mori H, Kobayashi S, Yamamoto A, Kodama E, Nakanishi Y, et al. Evaluation of in vitro proliferative activity of human fetal neural stem/progenitor cells using indirect measurements of viable cells based on cellular metabolic activity. J Neurosci Res 2002;69:869–79.
[20] Namiki J, Tator CH. Cell proliferation and nestin expression in the ependyma of the adult rat spinal cord after injury. J Neuropathol Exp Neurol 1999;58:489–98.
[21] Horner PJ, Power AE, Kempermann G, Kuhn HG, Palmer TD, Winkler J, et al. Proliferation and differentiation of progenitor cells throughout the intact adult rat spinal cord. J Neurosci 2000;20:2218–28.
[22] Shihabuddin LS, Horner PJ, Ray J, Gage FH. Adult spinal cord stem cells generate neurons after transplantation in the adult dentate gyrus. J Neurosci 2000;20:8727–35.
[23] Yamamoto S, Nagao M, Sugimori M, Kosako H, Nakatomi H, Yamamoto N, et al. Transcription factor expression and Notch-dependent regulation of neural progenitors in the adult rat spinal cord. J Neurosci 2001;21:9814–23.
[24] Chow SY, Moul J, Tobias CA, Himes BT, Liu Y, Obrocka M, et al. Characterization and intraspinal grafting of EGF/bFGF-dependent neurospheres derived from embryonic rat spinal cord. Brain Res 2000;874:87–106.
[25] Ogawa Y, Sawamoto K, Miyata T, Miyao S, Watanabe M, Toyama Y, et al. Transplantation of in vitro expanded fetal neural progenitor cells results in neurogenesis and functional recovery after spinal cord contusion injury in rats. J Neurosci Res 2002;69:925–33.
[26] McDonald JW, Liu XZ, Qu Y, Liu S, Mickey SK, Turetsky D, et al. Transplanted embryonic stem cells survive, differentiate and promote recovery in injured rat spinal cord. Nat Med 1999;5:1410–2.
[27] Vacanti MP, Leonard JL, Dore B, Bonassar LJ, Cao Y, Stachelek SJ, et al. Tissue-engineered spinal cord. Transpl Proc 2001;33:592–8.
[28] Ahmed S, Raynolds BA, Weiss S. BDNF enhances the differentiation but not the survival of CNS stem cell-derived neuronal precursors. J Neurosci 1995;15:5765–78.
[29] Ghosh A, Greenberg ME. Distinct roles for bFGF and NT-3 in the regulation of cortical neurogenesis. Neuron 1995;15:89–103.
[30] Johe KK, Hazel TG, Muller T, Dugich-Djordjevic MM, McKay RD. Single factors direct the differentiation of stem cells from the fetal and adult central nervous system. Genes Dev 1996;10:3129–40.
[31] Nakashima K, Yanagisawa M, Arakawa H, Kimura N, Hisatsune T, Kawabata M, et al. Synergistic signaling in fetal brain by STAT3–Smad 1 complex bridged by p300. Science 1999;284:479–82.
[32] Nakamura M, Bregman BS. Differences in neurotrophic factor gene expression profiles between neonate and adult rat spinal cord after injury. Exp Neurol 2001;169:407–15.
[33] Frisen J, Johansson CB, Torok C, Risling M, Lendahl U. Rapid, widespread, and long-lasting induction of nestin contributes to the generation of glial scar tissue after CNS injury. J Cell Biol 1995;131:453–64.
[34] Nakamura M, Houghtling RA, MacArthur L, Bayer BM, Bregman BS. Difference in cytokine gene expression profile between acutely and chronically injured adult rat spinal cord. Exp Neurol 2002 [in press].
[35] Bonni A, Sun Y, Nadal-Vicens M, Bhatt A, Frank DA, Rozovsky I, et al. Regulation of gliogenesis in the central nervous system by the Jak/Stat-signaling pathway. Science 1997;278:477–83.
[36] Okano H. Stem cell biology of the central nervous system. J Neurosci Res 2002;69:698–707.
[37] Miyoshi Y, Date I, Ohmoto T. Three-dimensional morphological study of microvascular regeneration in cavity wall of the rat cerebral cortex using the scanning electron microscope: implications for delayed neural grafting into brain cavities. Exp Neurol 1995;131:69–82.
[38] Miyoshi Y, Date I, Ohmoto T. Neovascularization of rat fetal neocortical grafts transplanted into a previously prepared cavity in the cerebral cortex: a three-dimensional morphological study using the scanning electron microscope. Brain Res 1995;681:131–40.
[39] Casella GT, Marcillo A, Bunge MB, Wood PM. New vascular tissue rapidly replaces neural parenchyma and vessels destroyed by a contusion injury to the rat spinal cord. Exp Neurol 2002;173:63–76.
[40] Gloster A, Wu W, Speelman A, Weiss S, Causing C, Pozniak C, et al. The Tα-1-tubulin promoter specifies gene expression as a function of neuronal growth and regeneration in transgenic mice. J Neurosci 1994;14:7319–30.
[41] Wang S, Wu H, Jiang J, Delohery TM, Isdell F, Goldman SA. Isolation of neuronal precursors by sorting embryonic forebrain transfected with GFP regulated by the Tα-1 tubulin promoter. Nat Biotechnol 1998;16:196–201.
[42] Roy NS, Wang S, Jiang L, Kang J, Restelli C, Fraser RAR, et al. In vitro neurogenesis by neural progenitor cells isolated from the adult human hippocampus. Nat Med 2000;6:271–8.
[43] Sawamoto K, Yamamoto A, Kawaguchi A, Yamaguchi M, Mori K, Goldman SA, et al. Visualization and direct isolation of neuronal progenitor cells by dual-color flow cytometric detection of fluorescent proteins. J Neurosci Res 2001;65:220–7.
[44] Bregman BS, Kunkel-Bagden E, Schnell L, Dai HN, Gao D, Schwab ME. Recovery from spinal cord injury mediated by antibodies to neurite growth inhibitors. Nature 1995;378:498–501.
[45] GrandPre T, Li S, Strittmatter SM. Nogo-66 receptor antagonist peptide promotes axonal regeneration. Nature 2002;417:547–51.
[46] Liu BP, Fournier A, GrandPre T, Strittmatter SM. Myelin-associated glycoprotein as a functional ligand for the nogo-66 receptor. Science 2002;297:1190–3.
[47] Garcia-Abreu J, Mendes FA, Onofre GR, De Freitas MS, Silva LC, Moura Neto V, et al. Contribution of heparan sulfate to the non-permissive role of the midline glia to the growth of midbrain neurites. Glia 2000;29:260–72.
[48] Blondel O, Collin C, McCarran WJ, Zhu S, Zamostiano R, Gozes I, et al. A glial-derived signal regulating neuronal differentiation. J Neurosci 2000;20:8012–20.
[49] Song H, Stevens CF, Gage FH. Astroglia induce neurogenesis from adult neural stem cells. Nature 2002;417:39–44.
[50] Cai D, Deng K, Mellado W, Lee J, Ratan R, Filbin M. Arginase I and polyamines act downstream from cyclic AMP in overcoming inhibition of axonal growth MAG and myelin in vitro. Neuron 2002;35:711–9.
[51] Olson L, Wingenfalk J, Josephson A, Greitz D, Klason TK, Ityotani T, et al. Experimental spinal cord injury models: prospective and repair strategies. In: Ikada Y, Oshima N, editors. Tissue engineering for therapeutic use 5. Amsterdam: Elsevier; 2001. p. 21–36.
[52] Olson L. Regeneration in adult central nervous system: experimental repair strategies. Nat Med 1997;3:1329–35.
[53] Okano H. Neural stem cells: progression of basic research and perspective for clinical application. Keio J Med 2002;51:115–28.

筋萎縮性側索硬化症

阿部康二

▣ はじめに

筋萎縮性側索硬化症(ALS)は，神経系の運動ニューロンを比較的，選択的かつ系統的に傷害し，進行性の筋萎縮を主症状とする疾患である．ALS発症者の5〜10%は家族性で遺伝歴を持っており(FALS)，1993年以来，第21番染色体長腕上のCu/ZnSOD遺伝子に点突然変異が続々と見出されたが，10年を経た今日でもまだ十分病態は解明されていないため，根治療法も確立していない．しかし目覚しい遺伝子細胞生物学の進歩に支えられて，再生医療のチャレンジが始まっている．

ALSに対する遺伝子治療

運動ニューロン細胞死を抑制することで，患者の症状進行遅延効果を目指した治療が行われている．神経栄養因子は神経細胞のアポトーシス抑制や生存維持の強力な作用があるため，ALS治療への応用が高く期待されている．これまでALSに試みられた神経栄養因子遺伝子治療は，CT-1, BDNF, NT-3, CNTF, GDNFなどである．Haaseによれば，pmnマウスに対するアデノウイルス組み込みCT-1, BDNF, NT-3, CNTF遺伝子の筋肉注射による治療の結果，もっとも生存期間延長効果があったのはNT-3であり，次いでCNTF, CT-1の順に有効で，BDNFは無効であった[1]．一方，筆者らによる変異SOD遺伝子導入マウスに対するGDNFを用いた筋肉内遺伝子治療によれば，臨床症状の進行抑制効果とともに，脊髄運動ニューロンの細胞死抑制効果(図A)が認められ，生存シグナルAktの保持効果も認められた(図B)．したがって神経栄養因子遺伝子治療によって，生存シグナルの保持により細胞死抑制効果があったものと考えられる[2]．

神経栄養因子については，遺伝子治療以外に直接これらの蛋白を投与することも可能である[3]．ALS患者に対するIGF-1の皮下注射やBDNFの髄腔内注入療法は，明らかな効果が見られなかったが[4]，IGF-1の脊髄腔内持続注入療法により，変異SOD導入マウス[5]およびALS患者の両方において進行抑制効果があることが分り，HGFなどとともに今後の発展が期待される．この他に合成フリーラジカルスカベンジャーであるedaravoneやAVSなどが，wobblerマウスの運動ニューロン細胞死抑制効果があったとされており[6]，immunophlinやmolecular chaperoneなどの可能性も含めて，再生治療にむけた研究進展が期待される．

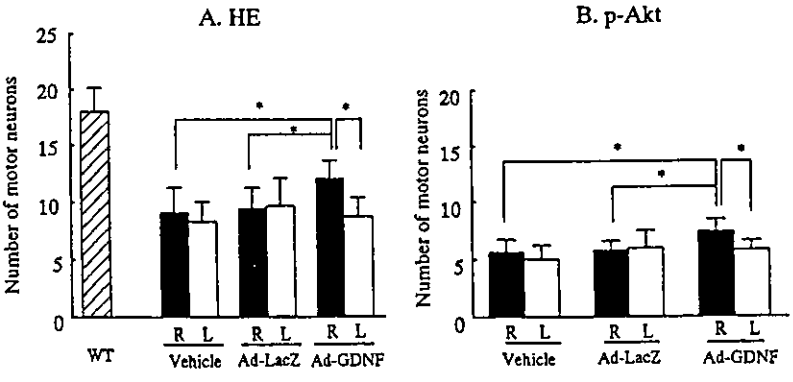

アデノウイルス組み込み神経栄養因子GDNFによるALSモデルマウス遺伝子治療効果

アデノウイルス組み込み神経栄養因子GDNF治療群の治療側(R：Ad-GDNF)の運動神経細胞残存率が高く(A)，生存シグナルp-Aktの陽性率も高い(B)ことがわかる．

ALSにおける内因性神経幹細胞の活性化

近年になり，成熟した中枢神経組織内にも分裂増殖可能な「幹細胞」が存在することが明らかにされてきて注目されている．筆者らの研究では，変異SOD導入マウス脊髄において神経幹細胞発達の3段階のうち，第1期(増殖期)のマーカーであるBrdUラベルされた細胞は，発症前後共に認められなかったが[7]，第2期(移動期)マーカーでもあるPSA-NCAMについては，発症以前から運動ニューロンで発現が認められた．しかしPSA-NCAMは神経幹細胞発達の，第2期以

あべ こうじ　岡山大学教授/大学院医歯学総合研究科神経病態内科学(神経内科)

0289-0585/03/¥500/論文/JCLS

外でも細胞接着因子として発現が見られることがあるので，BrdU ラベルされた細胞が観察されていない状況では，直ちに内因性神経幹細胞の活性化と断定することはできない．しかし変異 SOD 導入ラットにおいては，BrdU ラベルされた細胞が見出されたとする報告(割田ら)もあり，この相違が種差によるのかも含めて今後の検討が求められる．

幹細胞移植による ALS の再生治療

神経幹細胞を用いた ALS 再生治療のもう一つの可能性は移植であり，成熟脳由来細胞や ES 細胞などを用いて ALS 病巣に移植することが可能である．この際，培養中の幹細胞に特定の遺伝子を組み込むことも可能であり，あるいは組み込まずにそのまま移植することもできる[8]．それぞれの幹細胞には表に示したような特色があり，今後の ALS 治療に向けた検討が求められている．ボストンの Evan Snyder のグループは，すでに 2000 年には変異 SOD 導入マウス脊髄へ神経幹細胞を移植して，病変部位への生着や神経突起伸張を確認しており，フロリダのグループはヒト奇形腫細胞株(NTera 2/D 1)でも，移植により変異 SOD 導入マウス脊髄へ生着し，発症遅延効果と生存延長効果が認められたと報告している[9]．その後も多くのグループが先進的な研究を続けており，「Project ALS」と名づけられたハーバード・コーネル・コロンビア・ジョンスホプキンス 4 大学共同研究では，ES 細胞の一部を取り出して増殖させた EBD(embryoid body-derived)細胞により，ES 細胞のような腫瘍性増殖なく，安全にラット麻痺肢の運動能力改善を確認している[10]．このグループは，すでに 28 匹のアフリカ緑ザルを用いた安全性試験を始めており，近い将来のヒト臨床応用へと準備を進めている．

一方，ジョンスホプキンスの Gearhart らのグループは，sindbis ウイルスで脊髄運動ニューロンを傷害したラットの脊髄腔内に 100～150 万個のヒト幹細胞を注入するだけで，髄腔内を細胞が浮遊しながら注入数の約 6%の細胞が脊髄内に侵入して，神経細胞様の分化をしたと報告している[11,12]．このように，ALS への細胞移植による再生治療には大きな期待が寄せられるが，いくつかの重要な課題が残っている[11,13]．1 つ目は運動ニューロンへの分化誘導の確実性であり，2 つ目は移植した幹細胞から筋肉までの軸索伸長，3 つ目は軸索伸長先での幹細胞末梢と筋細胞とのネットワーク再構築という点，4 つ目は移植されたホスト脊髄内の細胞環境の問題であり，5 つ目は移植効果が移植細胞による栄養因子分泌を介した単なる細胞保護作用でしかないという批判をクリアすることである．特に第 4 の点は重要で，ALS の運動ニューロン細胞死における細胞選択性および進行性への脊髄内グリア細胞の関与は重要であるとされており，この点が解決されないといたずらに移植しても，すぐさま内在性運動ニューロンと同様の運命に陥る危険性も指摘されているところである[10]．解決必要な課題は山積しているが，このような再生医療のチャレンジが ALS のような進行性難病治療への将来的な突破口となることは期待されてよい．

幹細胞の種類と特徴

特徴項目	胎児由来神経幹細胞	成熟脳由来神経幹細胞	ES 細胞	骨髄細胞
増殖性	良好	良	最大	良
分化能	良	良好	最大	良
修飾性(遺伝子導入等)	良	良	良	良
移植方法	手術	手術	手術	動静脈注射
ホスト内移動性	良	良	良	良
組織構築性	良	良好	良	良
細胞安定供給性	?	良	良	最大
安全性	?	良好	腫瘍形成？	最良
臨床応用実現性	?	高い	?	最大

文　献

1) Haase G. Neurotrophic factor gene therapy for motor neuron disease. In : Abe K, editor. Molecular mechanism and therapeutics of ALS. Int Cong Series 1221. Amsterdam : Excerpta Medica : 2001. p. 317-24.
2) Manabe Y, Nagano I, Gazi MSA, et al. Adenovirus-mediated gene transfer of GDNF prevents motor neuron loss of transgenic model mice for ALS. Apoptosis 2002 ; 7 : 329-34.
3) Manabe Y, Nagano I, Gazi MSA, et al. GDNF protein prevents motor neuron loss of transgenic mode mice for ALS. Neurol Res 2003 ; 25 : 195-200.
4) Mitsumoto H. BDNF treatment in amyotrophic lateral sclerosis. In : Abe K, editor. Molecular mechanism and therapeutics of ALS. Int Cong Series 1221. Amsterdam : Excerpta Medica : 2001. p. 365-74
5) Nagano I, Siote M, Murakami T, et al. Positive effect of intrathecal IGF-1 for mutant SOD 1 transgenic mice model of ALS. 2003. in submission.
6) Ikeda K, Iwasaki Y, Kinoshita M. Treatment of wobbler mice with free radical scavenger. In : Abe K, editor. Molecular mechanism and therapeutics of ALS. Int Cong Series 1221. Amsterdam : Excerpta Medica ; 2001. p. 335-40.
7) Warita H, Murakami T, Manabe Y, et al. Induction of PSA-NCAM in surviving motoneurons of transgenic ALS mice. Neurosci Lett 2001 ; 300 : 75-8.
8) Abe A. Therapeutic potential of neurotrophic factors and neural stem cells against ischemic brain injury. J Cereb Blood Flow Metabol 2000 ; 20 : 1393-408.
9) Garbuzova-Davis S, Willing AE, Milliken M, et al. Positive effect of transplantation of hNT neurons(NTera 2/D 1 cell-line)in amodel of familial amyotrophic lateral sclerosis. Exp Neurol 2002 ; 174 : 169-80.
10) Holden C. Versatile cells against intractable diseases. Science 2002 ; 297 : 500-2.
11) Vastag B. Stem cells step closer to the clinic ; paralysis partially reversed in rats with ALS-like disease. JAMA 2001 ; 285 : 1691-3.
12) Janson CG, Ramesh TM, During MJ, et al. Human intrathecal transplantation of peripheral blood stem cells in amyotrophic lateral sclerosis. J Hematother Stem Cell Res 2001 ; 10 : 913-5.
13) Silani V, Fogh I, Ratti A, et al. Stem cells in the treatment of amyotrophic lateral sclerosis(ALS). Amyotroph Lateral Scler Other Motor Neuron Disord 2002 ; 3 : 173-81.

Original Paper

Neuropsychobiology

Neuropsychobiology 2005;51:34–38
DOI: 10.1159/000082853

Published online: December 20, 2004

Anxiolytic Effect of Hepatocyte Growth Factor Infused into Rat Brain

Koichi Isogawa[a] Jotaro Akiyoshi[a] Kensuke Kodama[a] Hirotaka Matsushita[a]
Takashi Tsutsumi[a] Hiroshi Funakoshi[b] Toshikazu Nakamura[b]

[a]Department of Neuropsychiatry, Oita University Faculty of Medicine, Oita, and [b]Division of Biochemistry, Department of Oncology, Biomedical Research Center, Osaka University Medical School, Osaka, Japan

Key Words
Anxiety · Hepatocyte growth factor · Rat

Abstract
Background: Hepatocyte growth factor (HGF) has the capacity to selectively direct thalamocortical projections into an intermediate target, the pallidum, and eventually to their final cortical destination. HGF may have a role in the mediation of anxiety. Very little is known about other central behavioral effects of HGF. ***Objective:*** Our aim was to determine what effect HGF has on anxiety in rats. ***Methods:*** HGF was infused at a constant rate into cerebral lateral ventricles and its effect on anxiety in rats was monitored. ***Results:*** In the elevated plus maze test and the black and white box test, HGF administration caused all indicators of anxiety to increase. No significant effect on general locomotor activity was seen. ***Conclusion:*** HGF infusion into the brain produces an anxiolytic effect.

Introduction

Hepatocyte growth factor (HGF) is a potent angiogenic growth factor [1–3]. Recently, it has been reported that HGF is induced in neurons during ischemia [4] and that HGF is neuroprotective against postischemic delayed neuronal death in the hippocampus [5, 6].

In the brain, HGF is expressed by specific classes of neurons in addition to nonneuronal cells in the ependyma and choroid plexus [7]. In contrast to HGF, c-Met transcripts have been predominantly localized in neurons of the cerebral cortex, hippocampus and septum [8–10]. HGF elevated the proto-oncogene c-*fos* mRNA in cultured septal neurons, showing a functional interaction between c-Met and its ligand [10]. This result, together with the presence of c-Met in the developing brain, raised the possibility that HGF may have a neurotrophic activity on central neurons. In keeping with this hypothesis, Hamanoue et al. [11] showed that HGF promoted the survival of cultured mesencephalic tyrosine hydroxylase-positive neurons. HGF acts on calbindin-D-containing hippocampal neurons and increases their neurite outgrowth, suggesting that HGF plays an important role in the maturation and function of hippocampal neurons [12]. Transfection of HGF gene into the subarachnoid space prevent-

KARGER
Fax + 41 61 306 12 34
E-Mail karger@karger.ch
www.karger.com

0302–282X/05/0511–0034$22.00/0

Accessible online at:
www.karger.com/nps

Jotaro Akiyoshi
Department of Neuropsychiatry
Oita University Faculty of Medicine
Hasama-Machi, Oita 879-5593 (Japan)
Tel. +81 97 586 5823, Fax +81 97 549 3583, E-Mail akiyoshi@med.oita-u.ac.jp

ed delayed neuronal death, accompanied by a significant increase in HGF in the cerebrospinal fluid (CSF). Prevention of delayed neuronal death by HGF is due to the inhibition of apoptosis through the blockade of bax translocation from the cytoplasm to the nucleus. HGF gene transfer into the subarachnoid space may provide a new therapeutic strategy for cerebrovascular disease [13].

HGF has the capacity to selectively direct thalamocortical projections into an intermediate target, the pallidum, and eventually to their final cortical destination [14]. Mice with a targeted mutation of the gene encoding urokinase plasminogen activator receptor (uPAR), a key component in HGF/scatter factor (SF) activation and function, have decreased levels of HGF/SF and a 50% reduction in neocortical GABAergic interneurons at embryonic and perinatal ages. Mice of the uPAR –/– strain survive until adulthood, and behavior testing demonstrates that they have an increased anxiety state [14]. HGF may have a role in the mediation of anxiety.

This is the first report to determine what effect HGF infused into cerebral lateral ventricles has on anxiety in rats.

Materials and Methods

Animals

Five-week-old male Wistar rats (Seack Yoshitomi Co., Fukuoka, Japan) were used for the present study. The number of rats was each 10 rats for experimental and control groups. The rats were housed in pairs for 3 weeks prior to the start of behavioral experiments in a sound-proof room at 24 ± 0.5 °C, 50 ± 5% relative humidity, with controlled 12-hour light-dark cycles (light from 18:00 to 6:00), and were allowed free access to food and water. The room was cleaned at random in a dim, red light. All testing was performed in July during the dark phase using a dim, red light. Animal care was in accordance with the guidelines for animal experimentation of Oita Medical University.

Surgical Procedures

Each rat was anesthetized with chloral hydrate (400 mg/kg, i.p.), a brain infusion cannula (brain infusion kit, model 1007D, Alzet Corp., Palo Alto, Calif., USA) was stereotactically implanted into the lateral cerebral ventricle (0.92 mm caudal and 1.6 mm lateral to the bregma and 3.5 mm deep), and a mini-osmotic pump (micro-osmotic pump, model 1003D; Alzet Corp.) was placed into subcutaneous tissue of the back. After the operation, rats were injected with ceftriaxone sodium (20 mg/kg, i.p.). Either HGF (30 μg) in the experimental group or a vehicle in the control group (Ringer's solution, pH = 7.4) was infused at a constant rate into the lateral ventricle of the rat via the micro-osmotic pump over a 3-day period. Tsuzuki et al. [15] reported that continuous intraventricular administration of the human recombinant HGF by using an osmotic mini-pump reduced the infarct volumes in the brain lesion and prevented apoptotic neuronal cell death.

Materials

A vehicle (Ringer's isotonic solution, pH 7.4) was used as a control. HGF was synthesized in the Division of Biochemistry, Department of Oncology, Biomedical Research Center, Osaka University Medical School.

Behavioral Testing

The first day of testing was concerned with measuring anxiety. All rats were subjected to the 'elevated plus maze', followed on the same day by the 'black and white box' test. Ethological measures in elevated plus maze comprised frequency scores for supported head dipping (exploratory movement of head/shoulders over the side of the maze), and stretched attend posture (exploratory posture in which the body is stretched forward then retracted to the original position without any forward locomotion). At the end of the day, rats received inescapable electric foot shocks to condition fear. On the second day, rats performed the conditioned fear test. Conditioned response models of fear and anxiety are based on classical procedures of fear conditioning [16]. On day 1 of fear conditioning, each rat was individually subjected to 5 min of inescapable electric foot shock (10 shocks of 1 s duration and 2 mA intensity, each shock separated by an interval of 40 s) in a chamber with a grid floor (31 × 30 × 25 cm). Twenty-four hours after the foot shock, the rats were again placed in the shock chamber and observed for 5 min without shocks. During the 5-min observation period, freezing behavior was recorded using a video camera. Every 10 s, the behavior was classified as either freezing or active. Freezing was defined as the absence of any observable movement of the body and/or vibrissae, aside from the movement necessitated by respiration. We also investigated general locomotor activity.

Elevated Plus Maze

The elevated plus maze consisted of two opposite open arms (50 × 10 cm) without side walls and two opposite enclosed arms (50 × 8 × 40 cm), and was elevated 50 cm above the floor. The rats were placed in the middle of the maze facing one of the open arms, and immediately left alone in the test room. They were observed and their responses were recorded for 300 s via a video camera. Five parameters were measured during 5 min: (1) time spent in the open arms, (2) total number of entries into the open arms, (3) number of stretched attend postures, and (4) number of head dips over the edge of the platform.

Black and White Box

The wall of the test box was 27 cm high, the size of each compartment was 23 × 27 cm, and the two compartments were connected by a 10-cm high semicircular hole. Both white and red light sources were 40 W, and the light sources were located 17 cm above the floor of the two compartments. The rats were placed in the center of the white compartment and the number of entries and time spent in the black and white compartments during 5 min were recorded. An entry into another compartment was scored whenever a rat placed all four paws in that compartment.

General Locomotor Activity

We investigated general locomotor activity of the rats by means of infrared photobeam breaks, since locomotion influences exploratory activity. The apparatus was 36 cm in height and the floor size was 30 × 30 cm. We measured the locomotor activity by photobeam breaks for 2 h.

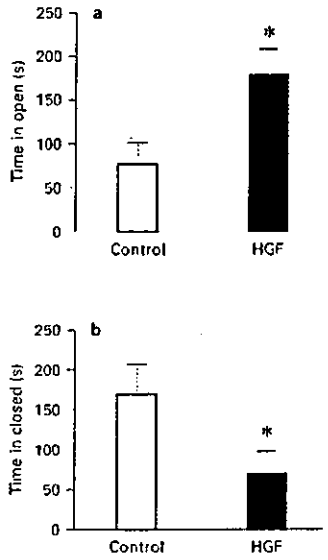

Fig. 1. **a** Time spent in the open arm of the elevated plus maze was significantly increased in the HGF-infused group compared to the control group. **b** Time spent in the closed arm of the elevated plus maze was significantly decreased in the HGF-infused group compared to the control group. * $p < 0.05$ vs. vehicle- and HGF-infused group.

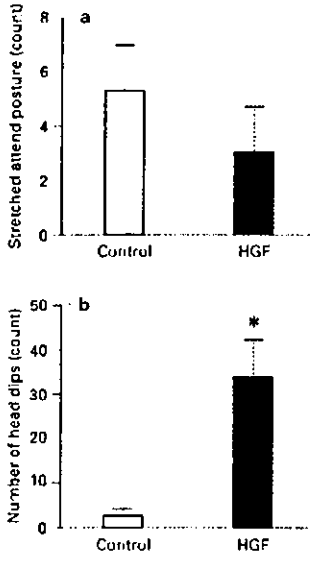

Fig. 2. **a** No effect of HGF or the control vehicle on the number of stretched attend postures in the elevated plus maze was seen. **b** The number of head dips in the elevated plus maze was significantly increased in the HGF-infused group compared to the control group. * $p < 0.05$ vs. vehicle- and HGF-infused group.

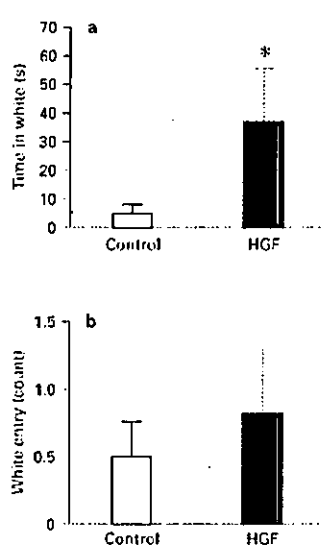

Fig. 3. In the black and white box test, the time spent in the white chamber was significantly increased in the HGF-infused group, compared to the controls (**a**). **b** No significant effect of HGF on the number of white chamber entries was seen. * $p < 0.05$ vs. vehicle- and HGF-infused group.

Statistical Analysis

The data were presented as means ± SE of the individual values from each group. Behavioral data (except for general locomotor activity) were analyzed using the Student t test for independent samples. The data of general locomotor activity were subjected to a two-way ANOVA. Statistical significance was accepted for $p < 0.05$.

Results

Time spent in the open arm of the elevated plus maze was significantly increased in the HGF-infused group, compared to the vehicle-treated group [$t(18) = 2.43$, $p < 0.031$; fig. 1a]. Time spent in the closed arm of the elevated plus maze was significantly decreased in the HGF-infused group compared to the control group [$t(18) = 2.23$, $p < 0.045$; fig. 1b]. No effect of HGF or the control vehicle on the number of stretched attend postures in the elevated plus maze was seen [$t(18) = 1.01$; fig. 2a]. The number of head dips in the elevated plus maze was significantly increased in the HGF-infused group compared to the control group. The number of head dips was significantly increased in the HGF-infused group compared to the vehicle-treated group [$t(18) = 2.61$, $p < 0.023$; fig. 2b]. In the black and white box test, the time spent in the white chamber was significantly decreased in the HGF-infused group, compared to the controls [$t(18) = 2.25$, $p < 0.048$; fig. 3a]. No significant effect of HGF on the number of white chamber entries was seen [$t(18) = 0.65$; fig. 3b]. The amount of conditioned fear stress-induced freezing behavior was significantly decreased in the HGF-infused group compared to the vehicle-treated group [$t(18) = 2.38$, $p < 0.036$; fig. 4]. No significant differences between the two groups were seen in general locomotor activity ($F_{2,35} = 1.30$; fig. 5).

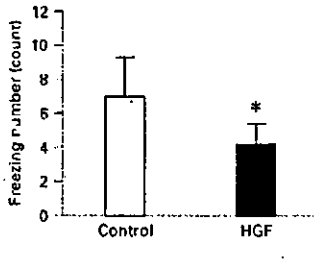

Fig. 4. Level of freezing induced by conditioned fear was significantly decreased in the HGF-infused group, compared to the controls. * $p < 0.05$ vs. vehicle- and HGF-infused group.

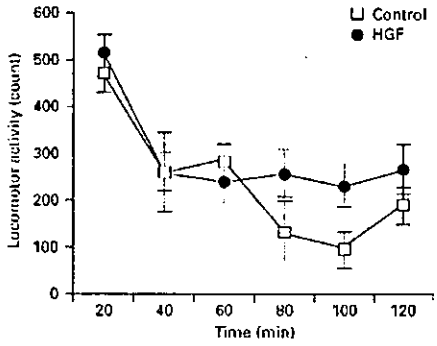

Fig. 5. No significant effect of HGF on general locomotor activity (number of photobeam breaks) was seen. Data are means ± SEM.

Discussion

This study provides the first evidence that HGF has an anxiolytic effect on the rat. HGF infusion into a lateral ventricle decreased anxiety as measured in the elevated plus maze and black and white box tests.

HGF was originally known as a cell mitogen and motogen, and has since been found to be a multifunctional growth factor with a variety of biological activities in numerous types of cells [17, 18]. The variety of biological functions attributed to HGF results from its interaction with its only known high-affinity transmembrane receptor, c-Met tyrosine kinase, present on target cells including central neurons [10, 19]. Coexpression of c-Met and HGF is oncogenic, and has been implicated in the progression of certain malignancies, in part, by decreasing tumor cell death and apoptosis [20, 21]. HGF and c-Met have been found to be present in specific subtypes of hippocampal neurons, cortex, septum, and cerebellum of both developing and adult mammalian brains [10, 12], but few reports exist concerning the biological activity of HGF in the CNS. A HGF-activating protease, HGF activator (HGFA), has recently been identified as a key enzyme that regulates the activity of HGF in vivo. HGFA appears to be associated with the cell surface. The HGFA antibody stained only astrocytes in the white matter in all the brain tissues. Expression of the mRNAs of HGF and HGFA was also seen in white matter astrocytes [22]. Recent studies have recognized effects of HGF on motor neuron survival, development and maturation, and on the function of cortical and hippocampal neurons in the developing brain [11, 12]. Tsuboi et al. [23] reported that consistent with the immunohistochemical data, a significantly higher concentration of HGF in Alzheimer's disease (AD) CSF was found as compared with controls. A significant correlation was also seen between CSF HGF levels and white matter high-signal foci determined on brain magnetic resonance imaging in AD patients. CSF HGF levels correspond with the white matter damage in AD brain [23].

Treatment with HGF induced an anxiolytic effect. But the mechanism of action of HGF has not been elucidated. The c-Met receptor has a heterodimeric protein which contains intracellular tyrosine kinase domains. Binding of HGF to c-Met might induce the anxiolytic effect [24]. HGF has the capacity to selectively direct thalamocortical projections into an intermediate target, the pallidum, and eventually to their final cortical destination. Mice with a targeted mutation of the gene encoding uPAR, a key component in HGF/SF activation and function, have decreased levels of HGF/SF and a 50% reduction in neocortical GABAergic interneurons at embryonic and perinatal ages. Mice of the uPAR −/− strain survive until adulthood, and behavior testing demonstrates that they have an increased anxiety state [14]. HGF may have a role in the mediation of anxiety.

In summary, this study reports that HGF infusion into the brain produced an anxiolytic effect in rats, as evaluated using the elevated plus maze, black and white box tests and conditioned fear test.

References

1 Aoki M, Morishita R, Taniyama Y, Kida I, Moriguchi A, Matsumoto K, Nakamura T, Kaneda Y, Higaki J, Ogihara T: Angiogenesis induced by hepatocyte growth factor in non-infarcted myocardium and infarcted myocardium: Up-regulation of essential transcription factor for angiogenesis. Gene Ther 2000;7: 417–427.

2 Hayashi S, Morishita R, Nakamura S, Yamamoto K, Moriguchi A, Nagano T, Taizi M, Noguchi H, Matsumoto K, Nakamura T, Higaki J, Ogihara T: Potential role of hepatocyte growth factor, a novel angiogenic growth factor, in peripheral arterial disease: Down-regulation of HGF in response to hypoxia in vascular cells. Circulation 1999;100:11301–11308.

3 Morishita R, Nakamura S, Hayashi S, Taniyama Y, Moriguchi A, Nagano T, Taiji M, Noguchi H, Takeshita S, Matsumoto K, Nakamura T, Higaki J, Ogihara T: Therapeutic angiogenesis induced by human recombinant hepatocyte growth factor in rabbit hind limb ischemia model as cytokine supplement therapy. Hypertension 1999;33:1379–1384.

4 Hayashi T, Abe K, Sakurai M, Itoyama Y: Inductions of hepatocyte growth factor and its activator in rat brain with permanent middle cerebral artery occlusion. Brain Res 1998;799: 311–316.

5 Miyazawa I, Matsumoto K, Ohmichi H, Katoh H, Yamashima I, Nakamura T: Protection of hippocampal neurons from ischemia-induced delayed neuronal death by hepatocyte growth factor: A novel neurotrophic factor. J Cereb Blood Flow Metab 1998;18:345–348.

6 Yamada T, Yoshiyama Y, Tsuboi Y, Shimomura T: Astroglial expression of hepatocyte growth factor and hepatocyte growth factor activator in human brain tissues. Brain Res 1997; 762:251–255.

7 Jung W, Castrén E, Odenthal M, Vande Woude G, Dienes HP, Lindholm D, Schirmacher P: Expression and functional interaction of hepatocyte growth factor-scatter factor (HGF-SF) and its receptor c-met in mammalian brain. J Cell Biol 1994;126:485–494.

8 Achim CL, Katyal S, Wiley CA, Shiratori M, Wang G, Oshika E, Petersen BE, Li J-M, Michalopoulos GK: Expression of HGF and c-met in the developing and adult brain. Brain Res Dev Brain Res 1997;102:299–303.

9 Honda S, Kagoshima M, Wanaka A, Tohyama M, Matsumoto K, Nakamura T: Localization and functional coupling of HGF and c-met/HGF receptor in rat brain: Implication as neurotrophic factor. Brain Res Mol Brain Res 1995;32:197–210.

10 Jung W, Castren E, Odenthal M, Vande Woude GF, Ishii T, Dienes HP, Lindholm D, Schirmacher P: Expression and functional interaction of hepatocyte growth factor-scatter factor and its receptor c-met in mammalian brain. J Cell Biol 1994;126:485–494.

11 Hamanoue M, Takemoto N, Matsumoto K, Nakamura T, Nakajima K, Kohsaka S: Neurotrophic effect of hepatocyte growth factor on central nervous system neurons in vitro. J Neurosci Res 1996;43:554–564.

12 Korhonen L, Sjoholm U, Takei N, Kero MA, Schirmacher P, Castren E, Lindholm D: Expression of c-Met in developing rat hippocampus: Evidence for HGF as a neurotrophic factor for calbindin D-expressing neurons. Eur J Neurosci 2000;12:3453–3461.

13 Hayashi K, Morishita R, Nakagami H, Yoshimura S, Hara A, Matsumoto K, Nakamura T, Kaneda Y, Ogihara T, Sakai N: Gene therapy for preventing neuronal death using hepatocyte growth factor: In vivo gene transfer of HGF to subarachnoid space prevents delayed neuronal death in gerbil hippocampal CA1 neurons. Gene Ther 2001;8:1167–1173.

14 Powell EM, Campbell DB, Stanwood GD, Davis C, Noebels JL, Levitt P: Genetic disruption of cortical interneuron development causes region- and GABA cell type-specific deficits, epilepsy, and behavioral dysfunction. J Neurosci 2003;23:622–631.

15 Tsuzuki N, Miyazawa T, Matsumoto K, Nakamura T, Shima K: Hepatocyte growth factor reduces the infarct volume after transient focal cerebral ischemia in rats. Neurol Res 2001;23: 417–424.

16 LeDoux JE: The Emotional Brain. New York, Simon and Schuster, 1996.

17 Rosen EM, Nigam SK, Goldberg ID: Scatter factor and the c-met receptor: A paradigm for mesenchymal epithelial interaction. J Cell Biol 1994;127:1783–1787.

18 Zarnegar R, Michalopoulos G: The many faces of hepatocyte growth factor: From hepatopoiesis to hematopoiesis. J Cell Biol 1995;129: 1177–1180.

19 Park M, Dean M, Kaul K, Braun MJ, Gonda MA, Vande Woude GF: Sequence of MET protooncogene cDNA has features characteristic of the tyrosine kinase family of growth-factor receptors. Proc Natl Acad Sci USA 1987;84: 6379–6383.

20 Bowers DC, Fan S, Walter K, Abounader R, Williams JA, Rosen EM, Laterra J: Scatter factor/hepatocyte growth factor activates AKT and protects against cytotoxic death in human glioblastoma via PI3-kinase and AKT-dependent pathways. Cancer Res 2000;60:4277–4283.

21 Fan S, Ma YX, Wang J, Yuan R, Meng Q, Cao Y, Laterra J, Goldberg ID, Rosen EM: The cytokine scatter factor inhibits apoptosis and enhances DNA repair by a common mechanism involving signaling through phosphatidyl inositol 3′ kinase. Oncogene 2000;19:2212–2223.

22 Yamada K, Moriguchi A, Morishita R, Aoki M, Nakamura Y, Mikami H, Oshima T, Ninomiya M, Kaneda Y, Higaki J, Ogihara T: Efficient oligonucleotide delivery using the HVJ-liposome method in the central nervous system. Am J Physiol 1996;271:R1212–R1220.

23 Tsuboi Y, Kakimoto K, Nakajima M, Akatsu H, Yamamoto T, Ogawa K, Ohnishi T, Daikuhara Y, Yamada T: Increased hepatocyte growth factor level in cerebrospinal fluid in Alzheimer's disease. Acta Neurol Scand 2003; 107:81–86.

24 Furge KA, Zhang YW, Vande Woude GF: Met receptor tyrosine kinase: Enhanced signaling through adapter proteins. Oncogene 2000;19: 5582–5589.

THE JOURNAL OF BIOLOGICAL CHEMISTRY
Vol. 279, No. 12, Issue of March 19, pp. 11327–11335, 2004
Printed in U.S.A.

NEDL1, a Novel Ubiquitin-protein Isopeptide Ligase for Dishevelled-1, Targets Mutant Superoxide Dismutase-1*

Received for publication, November 12, 2003, and in revised form, December 16, 2003
Published, JBC Papers in Press, December 18, 2003, DOI 10.1074/jbc.M312389200

Kou Miyazaki‡, Tomoyuki Fujita‡, Toshinori Ozaki‡, Chiaki Kato‡, Yuka Kurose‡, Maya Sakamoto‡, Shinsuke Kato§, Takeshi Goto¶, Yasuto Itoyama‖, Masashi Aoki‖, and Akira Nakagawara‡**

From the ‡Division of Biochemistry, Chiba Cancer Center Research Institute, Chiba 260-8717, Japan, the §Division of Neuropathology, Institute of Neurological Sciences, Faculty of Medicine, Tottori University, Yonago 683-8504, Japan, ¶Hisamitsu Pharmaceutical Company Incorporated, Tokyo 100-622, Japan, and the ‖Department of Neurology, Tohoku University School of Medicine, Sendai 980-8574, Japan

Approximately 20% of familial amyotrophic lateral sclerosis (FALS) arises from germ-line mutations in the superoxide dismutase-1 (*SOD1*) gene. However, the molecular mechanisms underlying the process have been elusive. Here, we show that a neuronal homologous to E6AP carboxyl terminus (HECT)-type ubiquitin-protein isopeptide ligase (NEDL1) physically binds translocon-associated protein-δ and also binds and ubiquitinates mutant (but not wild-type) SOD1 proportionately to the disease severity caused by that particular mutant. Immunohistochemically, NEDL1 is present in the central region of the Lewy body-like hyaline inclusions in the spinal cord ventral horn motor neurons of both FALS patients and mutant *SOD1* transgenic mice. Two-hybrid screening for the physiological targets of NEDL1 has identified Dishevelled-1, one of the key transducers in the Wnt signaling pathway. Mutant SOD1 also interacted with Dishevelled-1 in the presence of NEDL1 and caused its dysfunction. Thus, our results suggest that an adverse interaction among misfolded SOD1, NEDL1, translocon-associated protein-δ, and Dishevelled-1 forms a ubiquitinated protein complex that is included in potentially cytotoxic protein aggregates and that mutually affects their functions, leading to motor neuron death in FALS.

Amyotrophic lateral sclerosis (ALS)[1] is a progressive, fatal, neurodegenerative disease that is characterized by selective loss of motor neurons in the spinal cord, brain stem, and motor cortex. The sporadic and familial forms of the disease have similar clinical and pathological features. About 10% of ALS cases are familial, and mutation of superoxide dismutase-1 (SOD1) is found in 20% of familial ALS (FALS) patients (1, 2). Mice that express mutant *SOD1* transgenes develop an age-dependent ALS phenotype independent of levels of dismutase activity, suggesting that FALS pathology is because of a toxic gain of function in SOD1 and that the abnormal protein structure of mutant SOD1 is critical in the pathogenesis of motor neuron death (3–6). Recently, proteasome expression and activity have been reported to decrease with age in the spinal cord (7, 8). Furthermore, mutant SOD1 turns over more rapidly than wild-type SOD1, and an inhibitor of proteasome action inhibits this turnover and thus selectively increases the steady-state level of mutant SOD1 (8). These results suggest the involvement of the ubiquitin-proteasome function in the cause of FALS. However, the biochemical nature of this gain-of-function mutation in SOD1 and the mechanism by which SOD1 mutations cause the degeneration of motor neurons have remained elusive.

We show here the identification of a novel HECT-type ubiquitin-protein isopeptide ligase (E3), NEDL1, which is expressed in neuronal tissues, including the spinal cord, and selectively binds to and ubiquitinates mutant (but not wild-type) SOD1. NEDL1 is physically associated with translocon-associated protein-δ (TRAP-δ), one of the endoplasmic reticulum (ER) translocon components that has previously been reported to bind mutant SOD1 (9, 10). Both NEDL1 and TRAP-δ form a complex with mutant SOD1, with the binding intensity among these proteins being roughly proportionate to the rapidity of progression of the associated FALS phenotype. Immunohistochemical study has shown that NEDL1 is positive in the Lewy body-like hyaline inclusions in the spinal cord motor neurons of both FALS patients and mutant *SOD1* transgenic mice. We have also found that NEDL1 targets Dishevelled-1 (Dvl1) for ubiquitination-mediated degradation and that mutant (but not wild-type) SOD1 affects the function of Dvl1. Our observations suggest that NEDL1 is a quality control E3 that recognizes mutant SOD1 to form a tight complex with the physiological targets of NEDL1 in motor neurons of FALS patients.

EXPERIMENTAL PROCEDURES

Cell Culture and Transfection—Human neuroblastoma-derived cells were grown in RPMI 1640 medium supplemented with 10% heat-inactivated fetal bovine serum, 100 units/ml penicillin, and 100 μg/ml streptomycin. COS-7 and Neuro2a cells were maintained in Dulbecco's modified Eagle's medium supplemented with 10% heat-inactivated fe-

* This work was supported in part by Hisamitsu Pharmaceutical Co. Inc. (to A. N.), by grants from the Ministry of Health, Labor, and Welfare of Japan (to A. N. and Y. I.), and by grants from the Ministry of Education, Culture, Sports, Science, and Technology of Japan (to A. N., Y. I., and M. A.). The costs of publication of this article were defrayed in part by the payment of page charges. This article must therefore be hereby marked "*advertisement*" in accordance with 18 U.S.C. Section 1734 solely to indicate this fact.

The nucleotide sequence(s) reported in this paper has been submitted to the GenBank™/EBI Data Bank with accession number(s) AB048365 (Nbla0078 and human NEDL1), AB002320 (KIAA0322), and AB083710 (mouse Nedl1).

** To whom correspondence should be addressed: Div. of Biochemistry, Chiba Cancer Center Research Inst., 666-2 Nitona, Chuoh-ku, Chiba 260-8717, Japan. Tel.: 81-43-264-5431; Fax: 81-43-265-4459; E-mail: akiranak@chiba-ccri.chuo.chiba.jp.

[1] The abbreviations used are: ALS, amyotrophic lateral sclerosis; FALS, familial amyotrophic lateral sclerosis; SOD1, superoxide dismutase-1; E3, ubiquitin-protein isopeptide ligase; NEDL1, NEDD4-like ubiquitin-protein ligase-1; TRAP-δ, translocon-associated protein-δ; ER, endoplasmic reticulum; Dvl1, Dishevelled-1; RT, reverse transcription; LBHI, Lewy body-like hyaline inclusion; JNK, c-Jun N-terminal kinase; HECT domain, homologous to E6AP carboxyl-terminus.

tal bovine serum, 100 units/ml penicillin, and 100 μg/ml streptomycin. All cells were maintained in a humidified 37 °C incubator with 5% CO_2. All transfections were carried out with LipofectAMINE Plus transfection reagent (Invitrogen) according to the manufacturer's instructions. In some experiments, transfected cells were treated with MG-132 for 30 min at a final concentration of 40 μM.

RNA Analysis—A human multiple tissue mRNA blot and a fetal human multiple mRNA blot (Invitrogen) were hybridized with a ^{32}P-labeled ApaI-ScaI restriction fragment of *NEDL1* cDNA under standard conditions. For reverse transcription (RT)-PCR analysis, cDNA derived from adult human neural system (BioChain Institute, Hayward, CA) was subjected to PCR amplification using the following primers: *NEDL1*, 5′-CCGATTTGAGATCACTTCCTCC-3′ (sense) and 5′-CCGCTTTCCATCAGGTTGTT-3′ (antisense); and glyceraldehyde-3-phosphate dehydrogenase, 5′-ACCTGACCTGCCGTCTAGAA-3′ (sense) and 5′-TCCACCACCCTGTTGCTGTA-3′ (antisense). The amplified products were separated by electrophoresis on a 1.5% agarose gel and visualized by ethidium bromide post-staining. Amplification of glyceraldehyde-3-phosphate dehydrogenase was used as an internal control.

In Vitro Ubiquitination Assays—*In vitro* ubiquitination assays were performed as follows. Reaction mixtures containing 0.5 μg of purified glutathione *S*-transferase fusion proteins, 0.25 μg of yeast ubiquitin-activating enzyme (*E1*) (BostonBiochem, Cambridge, MA), 1 μl of crude lysates from *Escherichia coli* expressing ubiquitin carrier proteins (*E2*), and 10 μg of bovine ubiquitin (Sigma) were incubated in 250 mM Tris-HCl (pH 7.6), 1.2 M NaCl, 50 mM ATP, 10 mM $MgCl_2$, and 30 mM dithiothreitol. Reactions were terminated after 2 h at 30 °C by the addition of SDS sample buffer. Samples were resolved by SDS-PAGE, transferred to membranes, and immunoblotted with anti-ubiquitin monoclonal antibody 1B3 (Medical & Biological Laboratories, Nagoya, Japan).

Immunofluorescence Staining—Cells grown on coverslips were processed for immunofluorescence. Briefly, cells were fixed in 3.7% formaldehyde, permeabilized in 0.2% Triton X-100, and finally incubated with anti-NEDL1 antibody (diluted 1:100). The primary antibody was detected with fluorescein isothiocyanate-conjugated goat anti-rabbit IgG (diluted 1:500; Jackson ImmunoResearch Laboratories, Inc., West Grove, PA). Images were taken using an Olympus confocal microscopy system.

Yeast Two-hybrid Screening—Yeast two-hybrid screening was performed using the Gal4-based Matchmaker two-hybrid system with the cDNA libraries derived from fetal human brain (first screening) and adult human brain (second screening) (Clontech, Palo Alto, CA). *Saccharomyces cerevisiae* CG1945 cells were transformed with pAS2-1-NEDL1-1 (amino acids 757–1114; first screening) or pAS2-1-NEDL1-2 (amino acids 382–1448; second screening), which did not activate the transcription of *lacZ* alone. The transformants were subsequently transformed with the cDNA library, and the *lacZ*-positive colonies were selected. The plasmid DNAs were extracted from these positive colonies, and their nucleotide sequences were determined.

Immunoprecipitation and Western Blot Analysis—Anti-NEDL1 and anti-TRAP-δ polyclonal antibodies were raised in rabbits against an NEDL1 oligopeptide (amino acids 460–482) and a TRAP-δ oligopeptide (amino acids 93–126), respectively. For immunoprecipitation, COS-7 or Neuro2a cells were cotransfected with the expression plasmids in various combinations and lysed 48 h later in 10 mM Tris-HCl (pH 7.8), 150 mM NaCl, 1% Nonidet P-40, 1 mM EDTA, and 1 mM phenylmethylsulfonyl fluoride supplemented with protease inhibitor mixture (Sigma). Whole cell lysates were immunoprecipitated with anti-NEDL1, anti-FLAG (M2; Sigma), or anti-Myc (9B11; Cell Signaling Technology, Beverly, MA) antibody. Immune complexes were recovered on protein G-Sepharose beads, eluted by boiling in Laemmli sample buffer, electrophoresed on SDS-polyacrylamide gel, and then transferred to a polyvinylidene difluoride membrane (Immobilon, Millipore Corp., Bedford, MA) by electroblotting. For ubiquitination experiments, cell lysis was performed in radioimmune precipitation assay buffer (10 mM Tris-HCl (pH 7.4), 150 mM NaCl, 1% Nonidet P-40, 0.1% sodium deoxycholate, 0.1% SDS, and 1 mM EDTA), followed by strong sonication and freeze-thaw. The membrane was probed with the indicated primary antibodies and then incubated with the appropriate secondary antibodies labeled with horseradish peroxidase (Jackson ImmunoResearch Laboratories, Inc. and Southern Biotechnology Associates, Inc., Birmingham, AL). Immunoreactive bands were detected by the enhanced chemiluminescence technique (ECL, Amersham Biosciences). For the detection of c-Jun phosphorylation, we used anti-c-Jun (sc-45, Santa Cruz Biotechnology, Santa Cruz, CA) or anti-phospho-Ser^{63} c-Jun (Cell Signaling Technology) antibody.

Cloning of Human NEDL1 cDNA—A forward primer (5′-GGTTTTTAGGCCTGGCCGCC-3′) and a reverse primer (5′-CAATGAGGTACATGCCAATCC-3′) were used to amplify the 5′-part of the *NEDL1* cDNA using cDNA libraries derived from human neuroblastoma and fetal human brain (Stratagene, La Jolla, CA) as templates. The full-length human *NEDL1* cDNA was generated by fusion of the PCR-amplified fragment (nucleotides +1 to +68, where position +1 represents the translation initiation site) and the *KIAA0322* cDNA (a gift from T. Nagase, Kazusa DNA Institute). Gel electrophoresis and Western blot analysis were carried out as described above.

Expression Constructs—The mammalian expression plasmids for hemagglutinin-tagged and His_6-tagged ubiquitin were kind gifts of D. Bohmann. The full-length *NEDL1* cDNA was inserted into the mammalian expression plasmid pEF1/His (Invitrogen) or pIRESpuro2 (Clontech). cDNAs encoding wild-type and mutant forms of SOD1 were fused to the FLAG or Myc epitope tag sequence at their C termini and subcloned into pIRESpuro2. Similarly, the FLAG or Myc epitope tag sequence was attached to the C terminus of TRAP-δ. Also similarly, the FLAG or Myc epitope tag sequence was attached to the N terminus of Dvl1. Coding sequences were verified by automated DNA sequencing.

Protein Stability Experiments—Neuro2a cells were transfected with the expression plasmid for the wild-type or mutant form of SOD1 with or without the NEDL1 expression plasmid. Twenty-four hours after transfection, cycloheximide (50 μg/ml) was added to the culture medium, and the cells were harvested at the indicated time points by lysis in radioimmune precipitation assay buffer. The protein concentrations were determined using the Bradford protein assay system (Bio-Rad) according to the instructions of the manufacturer.

Immunohistochemistry—The immunohistochemical studies were performed as described previously using affinity-purified rabbit anti-NEDL1 antibody (11). Patient tissues were obtained at autopsy from two FALS siblings from a Japanese family. The clinical course of the sister, who died at age 46, was 18 months (case 1), and that of the brother, who died at age 65, was 11 years (case 2) (11). The *SOD1* gene was mutated with a 2-bp deletion at codon 126 (11, 12). Normal spinal cord tissues were obtained from three neurologically and neuropathologically normal individuals. The same study was performed on spinal cord tissues from three normal rats and a transgenic ALS rat carrying a mutant allele of the human *SOD1* gene (H46R) (13). These mice were killed at 180 days. As a negative control, some sections were incubated with anti-NEDL1 antibody that had been pre-absorbed with an excess of NEDL1 antigen. Bound antibodies were visualized by the avidin-biotin-immunoperoxidase complex method.

RESULTS

Cloning and Expression of the NEDL1 E3 Gene—To detect novel molecules that are important in regulating neuronal programmed cell death, we constructed oligo-capping cDNA libraries from a mixture of three fresh human neuroblastoma tissues (stages 1 and 2) that were undergoing gradual spontaneous regression, probably by neuronal apoptosis (14). Screening of 1152 novel genes by RT-PCR revealed that 194 genes were expressed differentially in regressing neuroblastomas with favorable prognosis and in aggressive tumors with poor prognosis. Among these genes, we found a partial cDNA sequence with an HECT-like domain (*Nbla0078*) that partially matched the *KIAA0322* gene. Because *KIAA0322* lacks a 5′-coding region, we used a genome-based PCR procedure to clone the corresponding full-length cDNA. This is predicted to encode a protein product of 1585 amino acids with homology to NEDD4 E3 (15, 16), which includes a C2 domain at the N-terminal region supposed to mediate its membrane localization in a calcium-dependent manner, two WW motifs important for protein-protein interaction through binding to specific proline-rich clusters, and a conserved catalytic HECT domain at the C terminus (Fig. 1*A*). We named this novel ligase, which mapped to chromosome 7p13, NEDL1 (NEDD4-like ubiquitin-protein ligase-1). We also cloned the mouse counterpart of *NEDL1* cDNA, whose amino acid sequence is 78% identical to the human sequence. Tissue-specific expression of *NEDL1* mRNA of ~10 and 7 kb in size was observed, with predominant expression in adult and fetal brains as examined by Northern blot analysis (Fig. 1*B*). Its

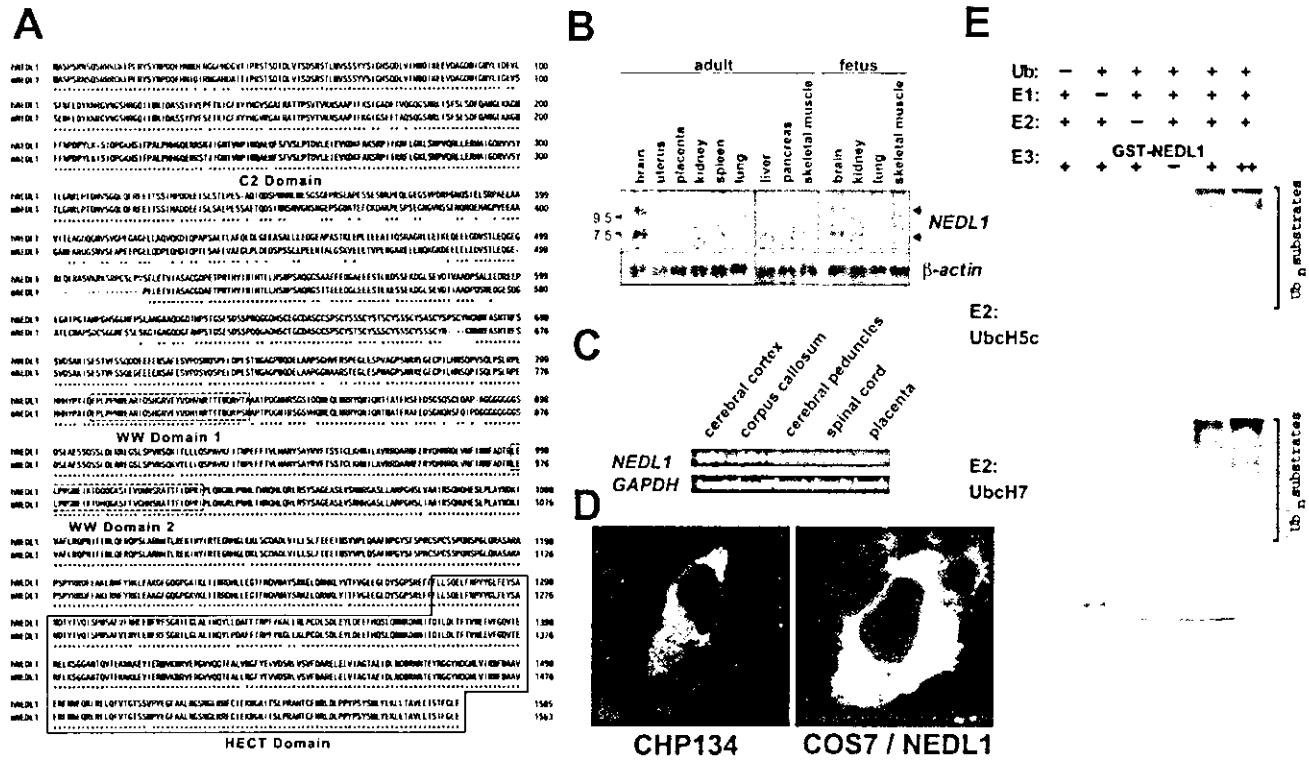

FIG. 1. **Amino acid sequence, brain-specific expression, and subcellular localization of NEDL1 E3.** *A*, alignment of conserved amino acid sequences of human NEDL1 (*hNEDL1*) and its mouse homolog (*mNEDL1*). *Numbers* on the right indicate the number of residues to the initiator methionine. The C2 domain (*shaded*), two WW domains (*dashed boxes*), and the HECT domain (*solid box*) are indicated. *B*, brain-specific expression of *NEDL1* mRNA. Total RNAs derived from the indicated adult (*left panel*) and fetal (*right panel*) human tissues were analyzed by Northern blotting using a ^{32}P-labeled human *NEDL1* cDNA restriction fragment as a probe. Control hybridization with a human β-actin cDNA probe verified the equal amount of RNA loaded. *C*, expression of *NEDL1* in human brain subsections. Total RNA from the cerebral cortex, corpus callosum, cerebral peduncles, spinal cord, or placenta was subjected to RT-PCR using specific primers for *NEDL1* or glyceraldehyde-3-phosphate dehydrogenase (*GAPDH*). RT-PCR analysis for *NEDL1* in the placenta provided a negative control. Amplification of glyceraldehyde-3-phosphate dehydrogenase was used as an internal control. *D*, confocal microscopic images of human neuroblastoma CHP134 cells (*left panel*) and COS-7 cells transfected with an expression plasmid for NEDL1 (*right panel*). Cells were subjected to immunofluorescence analysis using rabbit anti-NEDL1 polyclonal antibody, followed by fluorescein isothiocyanate-conjugated anti-mouse IgG. E, *in vitro* ubiquitination assays showing that NEDL1 has a ubiquitin-protein ligase activity. The degree of ubiquitination was increased in an NEDL1-dependent manner. In this assay, yeast ubiquitin-activating enzyme (*E1*), bacterially expressed ubiquitin carrier protein (*E2*; UbcH5C or UbcH7), and bacterial lysates were incubated in the presence or absence of increasing amounts of glutathione *S*-transferase (*GST*)-NEDL1. Polyubiquitinated bacterial proteins appeared to migrate in a high molecular mass complex. *Ub*, ubiquitin.

expression was also weakly detected in adult kidney, where the size of the expressed transcript appeared to be <7 kb. Expression of *NEDL1* in specific regions of the nervous system was further confirmed in the cerebral cortex, corpus callosum, cerebral peduncles, and spinal cord by RT-PCR (Fig. 1*C*). Thus, NEDL1 is a novel HECT-type E3 preferentially expressed in neuronal tissues, including the spinal cord. Using a specific anti-NEDL1 polyclonal antibody that we generated, we localized NEDL1 primarily to the cytoplasm in both intact human neuroblastoma CHP134 cells and COS-7 cells transiently expressing NEDL1 (Fig. 1*D*). The *in vitro* system containing UbcH5c or UbcH7 demonstrated that NEDL1 has a ubiquitin-protein ligase activity (Fig. 1*E*).

NEDL1 Physically Interacts with TRAP-δ and Mutant SOD1—We then sought protein-binding partners of NEDL1 by yeast two-hybrid screening using the region including two WW protein interaction domains (amino acids 757–1114) as bait. Of 96 positive clones subjected to DNA sequencing, one was a full-length cDNA for TRAP-δ; this was of considerable interest, as TRAP-δ was previously reported to bind mutant (G85R and G93A), but not wild-type, SOD1 (9). TRAP-δ is a protein component of the translocon in the ER membrane (10). We therefore examined the interaction among NEDL1, TRAP-δ, and SOD1 by an immunoprecipitation assay after cotransfecting the corresponding expression constructs into COS-7 cells. As shown in Fig. 2 (*A* and *B*), NEDL1 was physically associated with both exogenous and endogenous TRAP-δ probably through the region of two WW domains, as originally suggested by the result of two-hybrid screening. Surprisingly, NEDL1 bound to mutant (but not wild-type) SOD1 (Fig. 2*C*). Furthermore, the degree of binding between NEDL1 and different mutant SOD1 proteins was roughly proportionate to the rapidity of progression (time from clinical onset to death) of the associated FALS phenotype (17–23). For example, two mutant SOD1 proteins associated with an extremely rapid clinical course (C6F and A4V) interacted very strongly with NEDL1. By contrast, the binding of NEDL1 to other mutants was less striking and decreased proportionately to the falloff of disease severity corresponding to those mutants. Of further interest, like the NEDL1-mutant SOD1 interaction, the binding intensity between TRAP-δ and mutant SOD1 was also dependent on the disease severity (Fig. 2*D*). These observations suggest that NEDL1 and TRAP-δ are normally associated with each other, but that misfolded mutant SOD1 makes a complex with them. Such a complex is not formed with wild-type SOD1. The experiments using the *in vitro* translated proteins suggested that association of mutant SOD1 and TRAP-δ was direct (data not shown). It therefore appears that mutant SOD1 forms tightly bound protein complexes with NEDL1 and TRAP-δ and that the tightness of binding in the complex is determined in part by

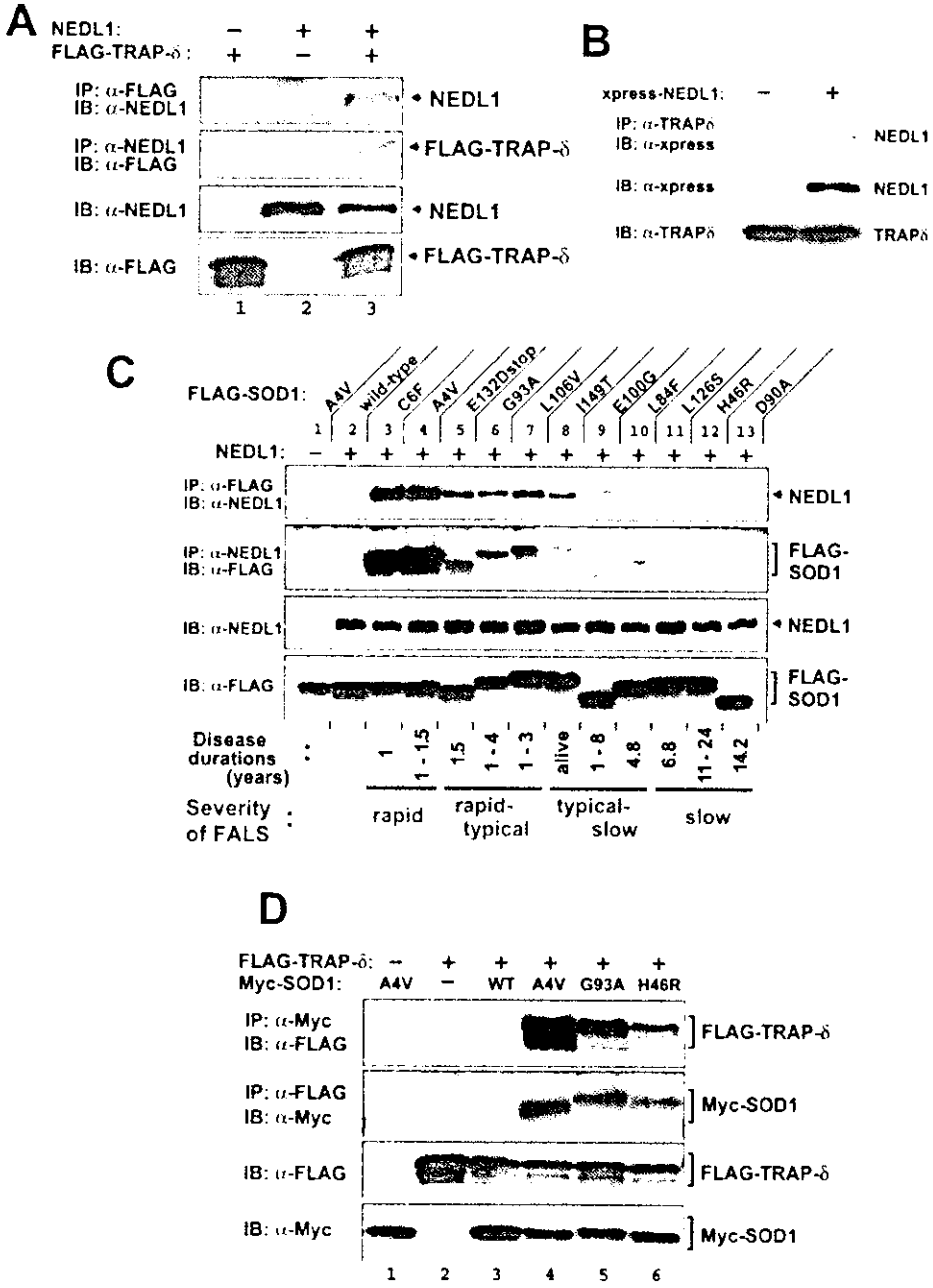

FIG. 2. **NEDL1 interacts with TRAP-δ and FALS-associated mutant forms of SOD1, but not with wild-type SOD1.** *A*, NEDL1 interacts with TRAP-δ. COS-7 cells were cotransfected with the indicated expression plasmids, and whole cell lysates were immunoprecipitated (*IP*) with anti-FLAG (*first panel*) or anti-NEDL1 (*second panel*) antibody. Immunoprecipitates were analyzed by immunoblotting (*IB*) using the indicated antibodies. Whole cell lysates were analyzed for expression levels of each protein by immunoblot analysis (*third* and *fourth panels*). Detection was performed with horseradish peroxidase-conjugated secondary antibodies. *B*, NEDL1 also binds to endogenous TRAP-δ. *C*, interaction between NEDL1 and mutant SOD1. Whole cell lysates from COS-7 cells overexpressing NEDL1 and one of the FLAG-tagged SOD1 mutants or wild-type SOD1 were immunoprecipitated with anti-FLAG (*first panel*) or anti-NEDL1 (*second panel*) antibody and then immunoblotted with anti-NEDL1 or anti-FLAG antibody, respectively. The expression of NEDL1 or FLAG-tagged SOD1 mutants was analyzed by immunoblotting using anti-NEDL1 (*third panel*) or anti-FLAG (*fourth panel*) antibody, respectively. Patients carrying the SOD1(C6F) and SOD1(A4V) mutations have a rapid clinical course, whereas mutant SOD1(L126S), SOD1(H46R), or SOD1(D90A) is associated with a slow clinical course. *D*, interaction of TRAP-δ with mutant SOD1. COS-7 cells were transiently cotransfected with the expression plasmid for FLAG-tagged TRAP-δ and the expression plasmid encoding one of the Myc-tagged SOD1 mutants or wild-type (*WT*) SOD1. Whole cell lysates were immunoprecipitated with anti-Myc (*first panel*) or anti-FLAG (*second panel*) antibody, followed by immunoblotting with anti-FLAG or anti-Myc antibody, respectively. The levels of overexpression of FLAG-tagged TRAP-δ (*third panel*) and Myc-tagged SOD1 (*fourth panel*) were analyzed by immunoblotting using anti-FLAG and anti-Myc antibodies, respectively.

properties of the mutant enzyme that also modulate disease severity of the resulting ALS phenotype. Such complexes do not form in cells with wild-type SOD1.

Determination of the Interaction Domains—We next examined the domains of NEDL1 required for formation of the SOD1·NEDL1·TRAP-δ complex. We generated various constructs of NEDL1 with deletions of each domain. Fig. 3 shows the results of immunoprecipitation assay for the association between deletion mutants of NEDL1 and mutant SOD1(G93A). Mutant SOD1 bound weakly to NEDL1 lacking WW domain-1 (Fig. 3*A*), suggesting that WW domain-1 and its surrounding portion are the region involved in their interaction. Immuno-

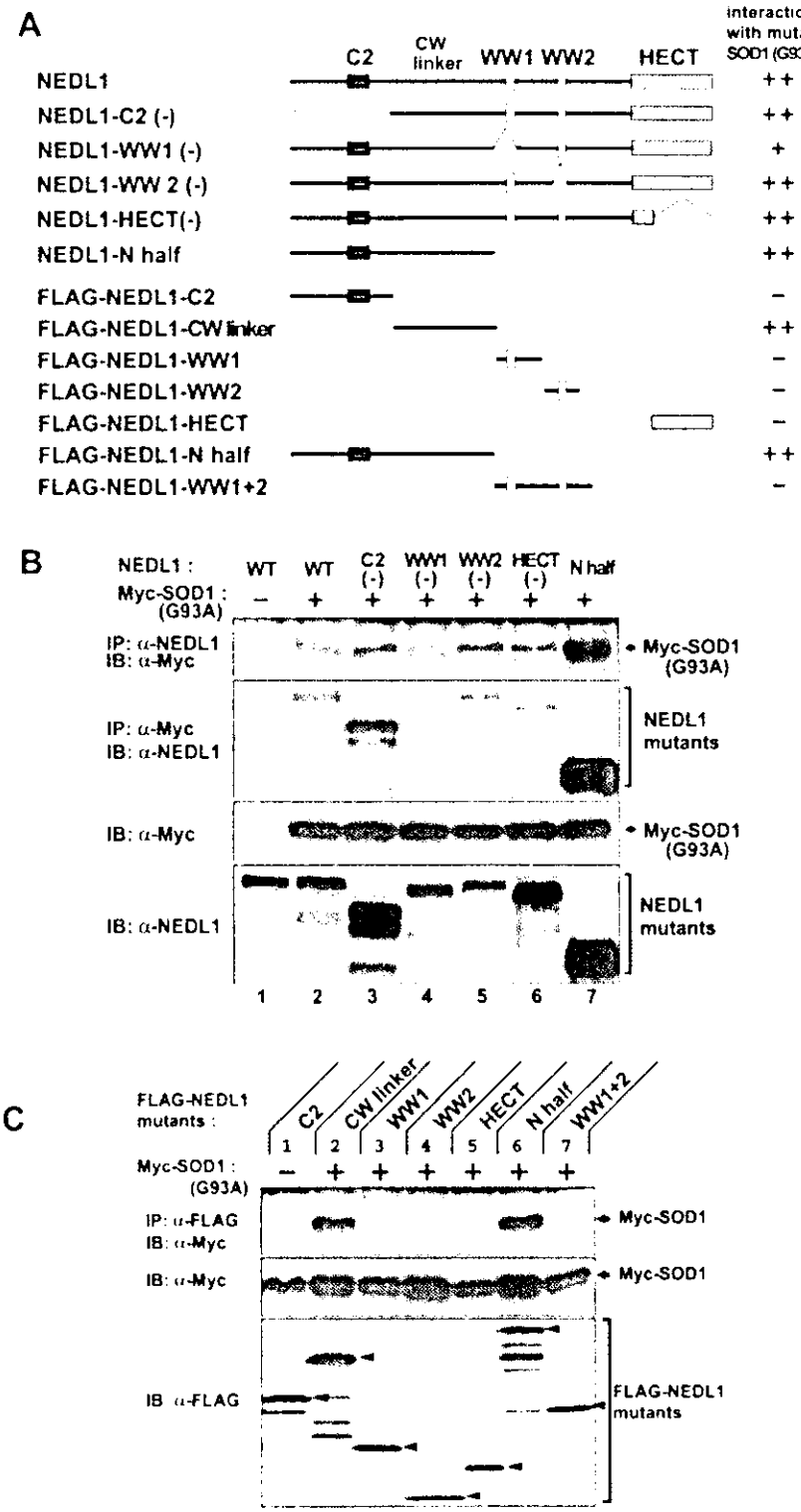

FIG. 3. **The region of NEDL1 between the C2 domain and WW domain-1 is required for interaction with mutant SOD1.** *A*, schematic illustration of wild-type NEDL1 and a series of deletion mutants of NEDL1. *CW linker* indicates the region between the C2 domain and WW domain-1 (*WW1*). *B* and *C*, immunoprecipitation and immunoblot analyses. In *B*, Myc-tagged mutant SOD1(G93A) was overexpressed together with wild-type (*WT*) NEDL1 or the indicated deletion mutants of NEDL1 in COS-7 cells. Whole cell lysates were immunoprecipitated (*IP*) with anti-NEDL1 (*first panel*) or anti-Myc (*second panel*) antibody, followed by immunoblotting (*IB*) with anti-Myc or anti-NEDL1 antibody, respectively. The expression levels of each protein were analyzed by immunoblotting using the indicated antibodies (*third* and *fourth panels*). In *C*, whole cell lysates were immunoprecipitated with anti-FLAG antibody and then immunoblotted with anti-Myc antibody (*upper panel*). Whole lysates were also analyzed by Western blotting for each protein (*middle* and *lower panels*).

precipitation analysis using the specific regions of NEDL1 clearly showed that the region between the C2 domain and WW domain-1 (CW linker region) is necessary for binding to mutant SOD1(G93A). Mutant SOD1(A4V) was also associated with NEDL1 through the same region, and TRAP-δ bound to the two WW domains of NEDL1 (data not shown).

NEDL1 Ubiquitinates Mutant SOD1 for Degradation Depending on the Disease Severity of FALS—Because NEDL1 is an E3, we next tested whether it ubiquitinates TRAP-δ and mutant SOD1 for degradation. As shown in Fig. 4*A*, NEDL1 clearly ubiquitinated mutant SOD1(A4V), but not TRAP-δ (data not shown). Furthermore, the degree of ubiquitination of mutant SOD1 by NEDL1 was dependent on the disease severity of FALS (A4V > G93A > H46R) (Fig. 4*A*). Fig. 4*B* shows the time course of degradation of wild-type and mutant SOD1 in the presence or absence of NEDL1. As reported previously (46), mutant SOD1 was degraded more rapidly than wild-type SOD1. NEDL1 did not affect wild-type SOD1 degradation. As expected from the co-immunoprecipitation and ubiquitination analyses, degradation of mutant SOD1 was stimulated by NEDL1 proportionately to the disease severity of FALS caused by the particular SOD1 mutant (A4V > G93A > H46R ≥

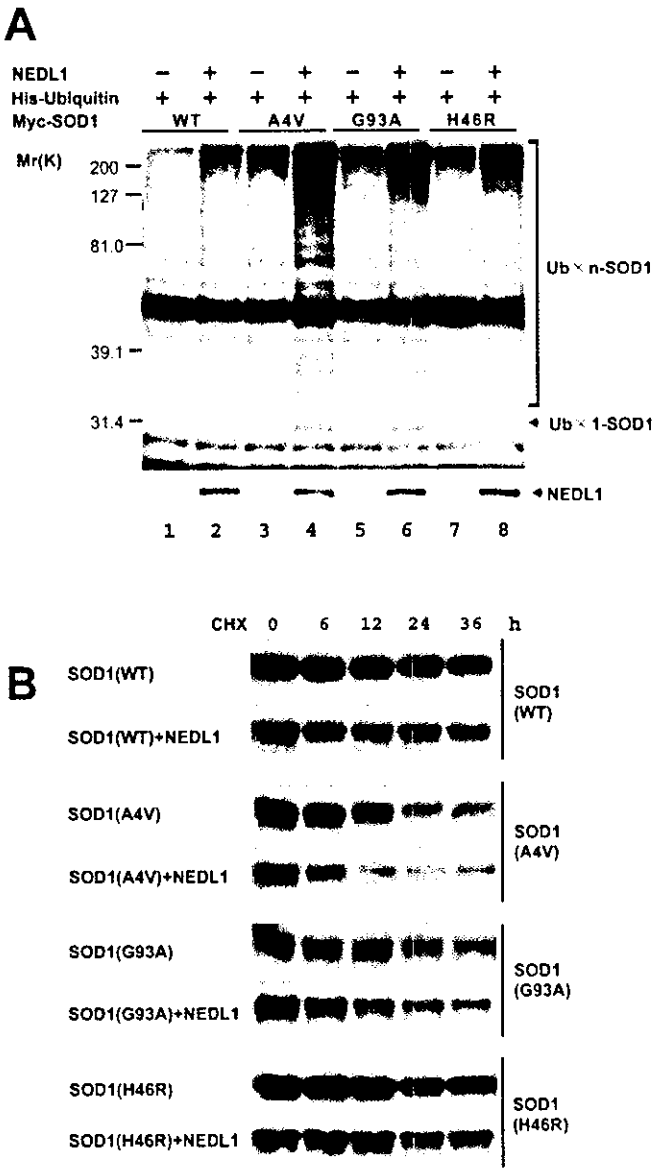

FIG. 4. **NEDL1-dependent ubiquitination and degradation of mutant forms of SOD1 correlate broadly with their respective clinical phenotypes.** *A*, NEDL1 ubiquitinates mutant SOD1 in a mutant type-dependent manner. COS-7 cells were transiently cotransfected with the indicated expression plasmids. Whole cell lysates from transfected COS-7 cells were immunoprecipitated with anti-Myc antibody, and immunoprecipitates were analyzed by Western blotting with anti-ubiquitin (*Ub*) antibody (*upper panel*). The *bracket* indicates slowly migrating ubiquitinated forms of SOD1. Whole cell lysates were analyzed by immunoblotting with anti-NEDL1 antibody to confirm the expression of transfected NEDL1 (*lower panel*). The running positions of molecular weight markers are indicated on the left. *B*, half-lives of wild-type (*WT*) and mutant SOD1 proteins in the presence or absence of NEDL1. Cell lysates were harvested from Neuro2a cells transfected with *SOD1* alone or with *SOD1* plus *NEDL1* at different time points as indicated after the addition of cycloheximide (*CHX*; final concentration of 50 μg/ml) and were analyzed for SOD1 protein levels by Western blotting with anti-FLAG antibody. In the presence of NEDL1, the half-lives of various mutant SOD1 proteins were reduced also roughly dependent on the disease severity of FALS (A4V > G93A > H46R).

wild-type). Thus, NEDL1 targeted mutant SOD1 for ubiquitin-mediated degradation in the cell in parallel with the binding intensity.

Immunohistochemistry—One of the characteristic cytopathological changes of mutant SOD1-linked FALS is the formation of neuronal Lewy body-like hyaline inclusions (LBHIs) that contain aggregates of SOD1 and ubiquitin (24). We therefore

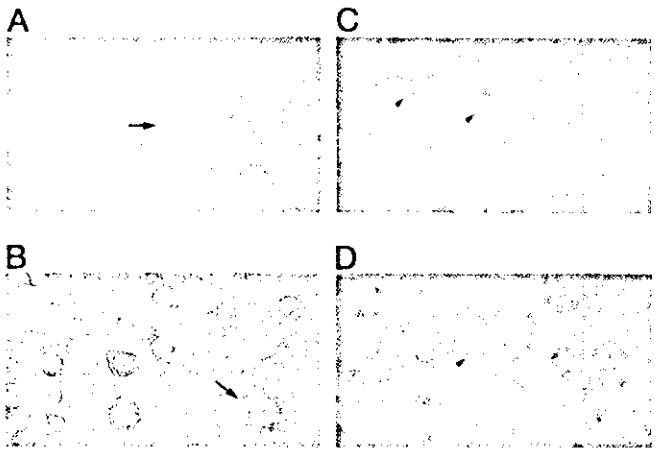

FIG. 5. **NEDL1 immunohistochemical analyses.** *A*, immunohistochemical analysis of NEDL1 in normal human spinal cord. NEDL1-positive anterior horn cells are evident (*arrow*), although the immunoreactivity for NEDL1 is somewhat faint. There was no counterstaining. Magnification ×520. *B*, NEDL1 immunohistochemistry in normal mouse spinal cord. Normal anterior horn cells are positive for NEDL1 (*arrow*). The section was counterstained with hematoxylin. Magnification ×750. *C*, immunostaining for NEDL1 in spinal cord LBHIs from an FALS patient with a frameshift 126 mutation in the *SOD1* gene. The NEDL1-positive reaction products were mostly restricted to the cores of the core and halo-type LBHIs (*arrowheads*). In the LBHI-bearing neurons and residual neurons, the antibody to NEDL1 also stained the neuronal cell body. There was no counterstaining. Magnification ×540. *D*, NEDL1 immunostaining in a spinal cord LBHI from an *SOD1*(H46R) transgenic mouse. An ill defined LBHI in the *SOD1*(H46R) transgenic mouse was positive for NEDL1; this ill defined LBHI shows a diffuse staining pattern (*arrowhead*). The staining intensity in the residual neurons stained by anti-NEDL1 antibody varied from neuron to neuron. The section was counterstained with hematoxylin. Magnification ×770.

performed immunostaining to determine whether the NEDL1 protein is included within the LBHIs of the spinal cord motor neurons obtained from two siblings with FALS caused by frameshift 126 mutation of SOD1 (11, 12). One case had neuropathological findings compatible with FALS with posterior column involvement, whereas the other had multisystem degeneration in addition to motor neuron disturbance. We also performed NEDL1 immunostaining in specimens obtained from mutant *SOD1*(H46R) transgenic mice at 180 days, by which time they show clinical motor signs in the hind limbs (13). The specificity of the NEDL1 staining was confirmed by pretreating the specimens with an excess of NEDL1 antigen. NEDL1 immunoreactivity in the spinal cords of the human control cases was identical to that of normal mice: immunoreactivity was identified predominantly in the cytoplasm of the neurons of the spinal cords (Fig. 5, *A* and *B*). The LBHIs in the anterior horn cells of two FALS patients and transgenic mice showed equivalent immunoreactivity for NEDL1. Although the intensity of NEDL1 immunoreactivity in neuronal LBHIs varied, most of the LBHIs were immunoreactive for NEDL1 (Fig. 5, *C* and *D*). The reaction products were generally restricted to the cores of the core and halo-type LBHIs that showed eosinophilic cores with pale peripheral halos upon hematoxylin and eosin staining (Fig. 5*C*); by contrast, immunopositive NEDL1 in ill defined LBHIs was distributed throughout the inclusions (Fig. 5*D*). NEDL1 immunoreactivity in the residual neurons in humans and mice was identified primarily in cell bodies. Thus, NEDL1 immunostaining was clearly positive in the FALS-related LBHIs that were also positive for ubiquitin and SOD1 (data not shown).

NEDL1 Targets Dishevelled-1 for Ubiquitin-mediated Protein Degradation—We next hypothesized that the physiological function of NEDL1 to mediate ubiquitination is interfered with

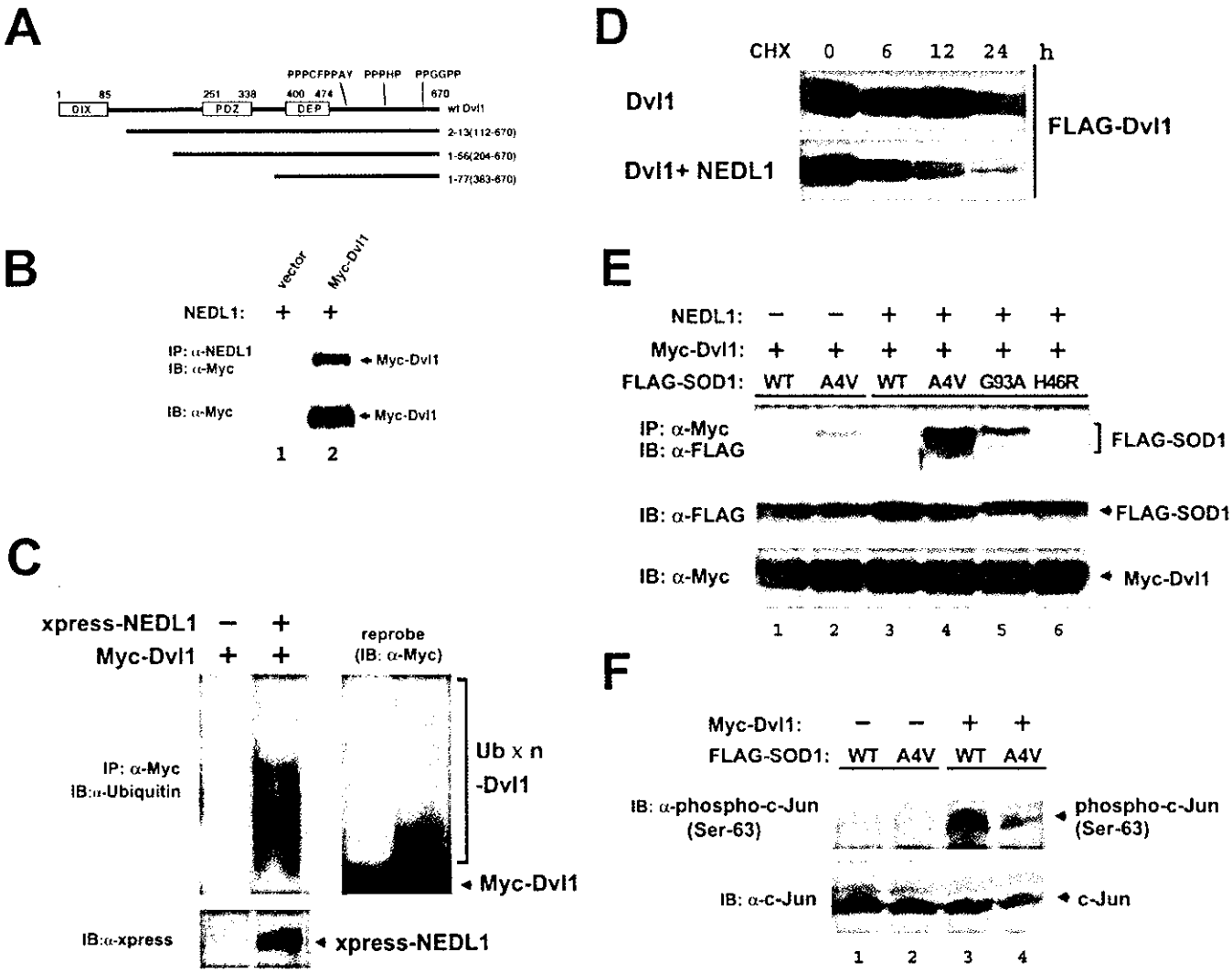

FIG. 6. **Dvl1 is a substrate of NEDL1, and its functions are disturbed by mutant SOD1(A4V).** *A*, schematic illustration of full-length Dvl1 and three clones obtained by yeast two-hybrid screening. Human Dvl1 consists of 670 amino acids and contains three conserved domains, including the DIX, PDZ, and DEP domains. Between the DEP domain and the C-terminal end, there are three proline-rich clusters, which might act as WW domain recognition sites. All three clones (clones 2–13, 1–56, 1–77) contain the DEP domain and these clusters. *B*, NEDL1 interacts with Dvl1. Myc-tagged Dvl1 was overexpressed together with NEDL1 in Neuro2a cells. Whole cell lysates were immunoprecipitated (*IP*) with anti-NEDL1 antibody, followed by immunoblotting (*IB*) with anti-Myc antibody (*upper panel*). The expression levels of Myc-tagged Dvl1 were analyzed by immunoblotting using anti-Myc antibody (*lower panel*). *C*, NEDL1 ubiquitinates Dvl1 in Neuro2a cells. The cells were transiently transfected with the indicated expression plasmids along with the ubiquitin expression plasmid in the presence or absence of the expression plasmid for XPRESS-tagged NEDL1. Whole cell lysates were immunoprecipitated with anti-Myc antibody and then immunoblotted with anti-ubiquitin antibody (*left panel*). The ladder of bands denoted by the *bracket* appeared to be ubiquitinated Dvl1. The expression of XPRESS-NEDL1 was analyzed by immunoblotting using anti-XPRESS antibody. The membrane was reprobed with anti-Myc antibody (*right panel*). *D*, Dvl1 is degraded by NEDL1. Neuro2a cells were transfected with the expression plasmid for FLAG-tagged Dvl1 with or without the NEDL1 expression plasmid. Transfected cells were harvested at different time points as indicated after the addition of cycloheximide (*CHX*; final concentration of 50 μg/ml), and Dvl1 protein levels were analyzed by Western blotting with anti-FLAG antibody. In the presence of NEDL1, the half-lives of FLAG-Dvl1 were significantly reduced. *E*, Dvl1 binds to mutant SOD1(A4V), and the degree of its binding is enhanced in the presence of NEDL1. Whole cell lysates prepared from COS-7 cells transfected with the indicated combinations of expression plasmids were subjected to immunoprecipitation and Western analyses as indicated. *F*, c-Jun phosphorylation by overexpression of Dvl1 is suppressed upon coexpression of mutant SOD1(A4V). Whole cell lysates from COS-7 cells transfected with the indicated combinations of expression plasmids were subjected to Western blotting with antibody against the phosphorylated form of c-Jun (*upper panel*) or with anti-c-Jun antibody (*lower panel*). *wt/WT*, wild-type.

by mutant SOD1. To test this hypothesis, we again performed yeast two-hybrid screening to obtain NEDL1-interacting molecules using the large region of NEDL1 (amino acids 382–1448) as bait. Of 396 His and β-galactosidase double-positive clones, 282 clones were subjected to DNA sequencing, and we identified Dvl1 (three clones). Human Dvl1 is a 670-amino acid protein with three conserved domains: a DIX domain, which is required for canonical Wnt/T-cell factor signaling; a PDZ domain, which is a target of both Stbm and casein kinase I binding; and a DEP domain, which is responsible for Dvl membrane localization during planar cell polarity signaling (25–27). Between the DEP domain and C-terminal end, there are three proline-rich clusters unique to mammalian Dvl1, which presumably act as the WW domain recognition sites. All three clones (clones 2–13, 1–56, and 1–77) contain the DEP domain and proline-rich clusters, suggesting that NEDL1 interacted with Dvl1 in the C-terminal half (Fig. 6*A*). In Neuro2a cells, NEDL1 co-immunoprecipitated with Dvl1 (Fig. 6*B*) and ubiquitinated it for degradation (Fig. 6, *C* and *D*). Thus, Dvl1 may be one of the physiological targets of NEDL1 E3. As recent studies strongly suggest that the cytotoxicity of SOD1 mutants is responsible for their aggregate properties, incorporating other proteins essential for cells into their aggregates (28), we examined the association between mutant SOD1 and Dvl1,

both of which interact with NEDL1. Of interest, Dvl1 bound to mutant SOD1(A4V), and complex formation was increased in the presence of NEDL1 roughly proportionately to the disease severity of FALS caused by the particular SOD1 mutant (Fig. 6*E*). Dvl1 is known to transduce not only the Wnt/β-catenin/T-cell factor pathway, but also the JNK/c-Jun pathway (27). Therefore, we next examined whether the Dvl1-induced phosphorylation of c-Jun at Ser^{63} was affected by the tight complex formation induced by inclusion of mutant SOD1. As shown in Fig. 6*F*, c-Jun phosphorylation induced by overexpression of Dvl1 was significantly suppressed by coexpression with mutant SOD1(A4V) in COS-7 cells.

DISCUSSION

Our present results demonstrate that a novel HECT-type NEDL1 E3, which is preferentially expressed in neuronal tissues, specifically targets mutant forms of SOD1 for ubiquitination-mediated protein degradation. NEDL1 is also associated with TRAP-δ localized at the ER translocon. The TRAP complex has recently been shown to facilitate the initiation of protein translocation in a substrate-specific manner (29). The NEDL1·TRAP-δ complex recognizes mutant (but not wild-type) SOD1, with a binding intensity that broadly parallels the disease severity of FALS. NEDL1 immunoreactivity was detected in the FALS-related LBHIs in the spinal cord ventral horn motor neurons, suggesting that, although mutant SOD1 is ubiquitinated for degradation by NEDL1, the mutant SOD1·NEDL1·TRAP-δ complex aggregates within the LBHIs. It is also conceivable that fragmentation of the Golgi apparatus reported in ALS patients and transgenic mice might be related to this aggregation (30, 31). These findings suggest possible hypotheses for the role of NEDL1 in the pathogenesis of FALS: 1) NEDL1, alone or with TRAP-δ, ubiquitinates and aggregates mutant SOD1, thereby decreasing the function of mutant SOD1; 2) NEDL1 and TRAP-δ form aggregates with mutant SOD1 that induce fragmentation of the Golgi apparatus, leading to neuronal apoptosis; 3) formation of these aggregates causes dysfunction of NEDL1 and/or TRAP-δ, and this, in turn, induces disturbances that ultimately cause motor neuron death; and 4) the mutant SOD1·NEDL1·TRAP-δ aggregates trap and inactivate unknown factor(s) such as molecular chaperones whose normal function is important for motor neuron viability.

To further understand the role of NEDL1 in motor neuron death, we searched for the physiological targets of NEDL1 and identified Dvl1. As expected, Dvl1 is ubiquitinated for degradation by NEDL1. Surprisingly, however, Dvl1 also interacts with mutant SOD1 in the presence of NEDL1 roughly proportionately to the disease severity of FALS caused by the particular SOD1 mutant. Dvl1, an essential multimodule signal transducer localized in the cellular cytosol and cytoskeleton, mediates planar cell polarity signaling as well as canonical Wnt/β-catenin signaling (27, 32). In mammals, three Dvl family members have so far been reported, and the level of Dvl1 expression is high in neuronal tissues (33). As far as we know, NEDL1 is the first E3 for Dvl1, interacting with the C-terminal region containing three proline-rich clusters. A recent report suggests that Dvl1 regulates microtubule stability through inhibition of glycogen synthase kinase-3β (34). Because cytoskeletal abnormalities have been reported in ALS motor neurons (35), it is possible that the effect of mutant SOD1 on NEDL1-mediated Dvl1 degradation is involved in the motor neuron death. Furthermore, Dvl1 is abundant in the postsynaptic membrane region at the neuromuscular junction (36) that is reported to be involved in several neurodegenerative disorders (37, 38). Of interest, *Dvl1* is mapped to chromosome 1p36, which is a commonly deleted region in many human cancers, including neuroblastoma (39). As NEDL1 is highly expressed in neuroblastomas with favorable prognosis, which have a tendency to differentiate and/or regress, NEDL1 may be involved in the regulation of neuronal differentiation and survival possibly by controlling Dvl1.

NEDL1, TRAP-δ, mutant SOD1, and Dvl1 appear to form a complex roughly proportionately to the disease severity of FALS caused by the particular SOD1 mutant. Our present observations strongly suggest that NEDL1 may be a quality control E3 recognizing misfolded mutant SOD1 (40). The association between mutant SOD1 and NEDL1 may induce the conformational change in the NEDL1 protein to increase the binding intensity with other physiological targets such as TRAP-δ (not ubiquitinated) and Dvl1 (ubiquitinated). This may lead to tight complex formation especially when the proteasome activity is impaired. It has been reported that the expression and function of proteasomes decrease with age in the spinal cord (7). Okado-Matsumoto and Fridovich (41) have also found that complex formation between mutant SOD1 and heat shock proteins leads to protein aggregates. Because our data show that the ER translocon component TRAP-δ is involved, aggregate formation may occur at the sites of the ER or Golgi apparatus or even at other cellular sites. The complex formation including NEDL1 and mutant SOD1 may conversely affect the physiological function of NEDL1, as demonstrated by a decrease in Dvl1-induced phosphorylation of c-Jun.

Recently, the RING finger-type E3 Dorfin has been reported to ubiquitinate mutant SOD1 for degradation (42). However, NEDL1 and Dorfin appear to be different in several aspects. First, NEDL1 is expressed specifically in neuronal tissues, including the spinal cord, whereas Dorfin is ubiquitously expressed in most human tissues. Second, both interaction between NEDL1 and mutant SOD1 and ubiquitination of the latter by NEDL1 roughly parallel the disease severity caused by the particular SOD1 mutant, whereas Dorfin similarly ubiquitinates mutant forms of SOD1. In addition, we have identified Dvl1 and TRAP-δ as cellular target proteins of NEDL1, whereas the physiological targets of Dorfin have never been reported. It is probable that there are some other E3 ligases targeting mutant SOD1. However, the molecular characteristics, including tissue-specific expression, subcellular localization, and age-dependent expression, might be important in the development of the FALS phenotype.

In conclusion, we have identified a novel neuronal E3 (NEDL1) that interacts with TRAP-δ and also binds to and ubiquitinates Dvl1 for degradation. Strikingly, NEDL1 targets and ubiquitinates mutant (but not wild-type) SOD1 for degradation. NEDL1 may normally function in the quality control of cellular proteins by eliminating misfolded proteins such as mutant SOD1, possibly via a mechanism analogous to that of ER-associated degradation (43–45). NEDL1 appears to complex tightly with mutant SOD1, Dvl1, and TRAP-δ, forming aggregates with species of mutant SOD1 that have escaped ubiquitin-mediated degradation. The NEDL1 function that affects the activities of the target proteins may also be modulated by mutant SOD1. All of these might contribute to the pathogenesis of FALS; further elucidation of the molecular mechanism of formation of this complex and its pathogenicity may provide insights into motor neuron death in ALS as well as possible new therapeutic strategies for ALS.

Acknowledgments—We thank Robert H. Brown, Jr. (Harvard Medical School) for critical comments and reading the manuscript. We also thank M. Ohira and Y. Nakamura for helping with cDNA cloning and sequencing; K. Watanabe and M. Suzuki for making plasmid constructs; M. Nagai and M. Kato for helping with immunohistochemical studies; S. Hatakeyama, M. Matsumoto, and K. Nakayama

for ubiquitination assay instruction; and S. Sakiyama for reading the manuscript.

REFERENCES

1. Rosen, D. R., Siddique, T., Patterson, D., Figlewicz, D. A., Sapp, P., Hentati, A., Donaldson, D., Goto, J., O'Regan, J. P., Deng, H. X., Rahmani, Z., Krizus, A., McKenna-Yasek, D., Cayabyab, A., Gaston, S. M., Berger, R., Tanzi, R. E., Halperin, J. J., Herzfeldt, B., van den Bergh, R., Hung, W.-Y., Bird, T., Deng, G., Mulder, D. W., Smyth, C., Laing, N. G., Soriano, E., Pericak-Vance, M. A., Haines, J., Rouleau, G. A., Gusella, J. S., Horvitz, H. R., and Brown, R. H., Jr. (1993) *Nature* **364,** 59–62
2. Deng, H. X., Hentati, A., Tainer, J. A., Iqbal, Z., Cayabyab, A., Hung, W.-Y., Getzoff, E. D., Hu, P., Herzfeldt, B., Roos, R. P., Warner, C., Deng, G., Soriano, E., Smyth, C., Parge, H. E., Ahmed, A., Roses, A. D., Hallewell, R., Rericak-Vance, M. A., and Siddique, T. (1993) *Science* **261,** 1047–1051
3. Cleveland, D. W., and Liu, J. (2001) *Nat. Med.* **6,** 1320–1321
4. Brown, R. H., Jr., and Robberecht, W. (2001) *Semin. Neurol.* **21,** 131–139
5. Cluskey, S., and Ramsden, D. B. (2001) *Mol. Pathol.* **54,** 386–392
6. Orrell, R. W., and Figlewicz, D. A. (2001) *Neurology* **57,** 9–17
7. Keller, J. N., Huang, F. F., and Markesbery, W. R. (2000) *Neuroscience* **98,** 149–156
8. Hoffman, E. K., Wilcox, H. M., Scott, R. W., and Siman, R. (1996) *J. Neurol. Sci.* **139,** 15–20
9. Kunst, C. B., Mezey, E., Brownstein, M. J., and Patterson, D. (1997) *Nat. Genet.* **15,** 91–94
10. Hartmann, E., Gorlich, D., Kostka, S., Otto, A., Kraft, R., Knespel, S., Burger, E., Rapoport, T. A., and Prehn, S. (1993) *Eur. J. Biochem.* **214,** 375–381
11. Kato, S., Shimoda, M., Watanabe, Y., Nakashima, K., Takahashi, K., and Ohama, E. (1996) *J. Neuropathol. Exp. Neurol.* **55,** 1089–1101
12. Kato, S., Hayashi, H., Nakashima, K., Nanba, E., Kato, M., Hirano, A., Nakano, I., Asayama, K., and Ohama, E. (1997) *Am. J. Pathol.* **151,** 611–620
13. Nagai, M., Aoki, M., Miyoshi, I., Kato, M., Pasinelli, P., Kasai, N., Brown, R. H., Jr., and Itoyama, Y. (2001) *J. Neurosci.* **21,** 9246–9254
14. Nakagawara, A. (1998) *Med. Pediatr. Oncol.* **31,** 113–115
15. Harvey, K. F., and Kumar, S. (1999) *Trends Cell Biol.* **9,** 166–169
16. Kumar, S., Tomooka, Y., and Noda, M. (1992) *Biochem. Biophys. Res. Commun.* **30,** 1155–1161
17. Kato, S., Takikawa, M., Nakashima, K., Hirano, A., Cleveland, D. W., Kusaka, H., Shibata, N., Kato, M., Nakano, I., and Ohama, E. (2000) *Amyotroph. Lateral Scler. Other Motor Neuron Disord.* **1,** 163–184
18. Orrell, R. W. (2000) *Neuromuscul. Disord.* **10,** 63–68
19. Cudkowicz, M. E., McKenna-Yasek, D., Sapp, P. E., Chin, W., Geller, B., Hayden, D. L., Schoenfeld, D. A., Hosler, B. A., Horvitz, H. R., and Brown, R. H., Jr. (1997) *Ann. Neurol.* **41,** 210–221
20. Ratovitski, T., Corson, L. B., Strain, J., Wong, P., Cleveland, D. W., Culotta, V. C., and Borchelt, D. R. (1999) *Hum. Mol. Genet.* **8,** 1451–1460
21. Aoki, M., Ogasawara, M., Matsubara, Y., Narisawa, K., Nakamura, S., Itoyama, Y., and Abe, K. (1993) *Nat. Genet.* **5,** 323–324
22. Kato, M., Aoki, M., Ohta, M., Nagai, M., Ishizaki, F., Nakamura, S., and Itoyama, Y. (2001) *Neurosci. Lett.* **312,** 165–168
23. Andersen, P. M., Forsgren, L., Binzer, M., Nilsson, P., Ala-Hurula, V., Keranen, M. L., Bergmark, L., Saarinen, A., Haltia, T., Tarvainen, I., Kinnunen, E., Udd, B., and Marklund, S. L. (1996) *Brain* **119,** 1153–1172
24. Shibata, N., Hirano, A., Kobayashi, M., Siddique, T., Deng, H. X., Hung, W.-Y., Kato, T., and Asayama, K. (1996) *J. Neuropathol. Exp. Neurol.* **55,** 481–490
25. Sussman, D. J., Klingensmith, J., Salinas, P., Adams, P. S., Nusse, R., and Perrimon, N. (1994) *Dev. Biol.* **166,** 73–86
26. Wodarz, A., and Nusse, R. (1998) *Annu. Rev. Cell Dev. Biol.* **14,** 59–88
27. Boutros, M., Paricio, N., Strutt, D. I., and Mlodzik, M. (1998) *Cell* **94,** 109–118
28. Julien, J. P. (2001) *Cell* **104,** 581–591
29. Fons, R. D., Bogert, B. A., and Hegde, R. S. (2003) *J. Cell Biol.* **160,** 529–539
30. Fujita, Y., Okamoto, K., Sakurai, A., Gonatas, N. K., and Hirano, A. (2000) *J. Neurol. Sci.* **174,** 137–140
31. Mourelatos, Z., Gonatas, N. K., Stieber, A., Gurney, M. E., and Dal Canto, M. C. (1996) *Proc. Natl. Acad. Sci. U. S. A.* **93,** 5472–5477
32. Wharton, K. A., Jr. (2003) *Dev. Biol.* **253,** 1–17
33. Tsang, M., Lijam, N., Yang, Y., Beier, D. R., Wynshaw-Boris, A., and Sussman, D. J. (1996) *Dev. Dyn.* **207,** 253–262
34. Krylova, O., Messenger, M. J., and Salinas, P. C. (2000) *J. Cell Biol.* **151,** 83–94
35. Julien, J. P., and Beaulieu, J. M. (2000) *J. Neurol. Sci.* **180,** 7–14
36. Luo, Z. G., Wang, Q., Zhou, J. Z., Wang, J., Luo, Z., Liu, M., He, X., Wynshaw-Boris, A., Xiong, W. C., Lu, B., and Mei, L. (2002) *Neuron* **35,** 489–505
37. De Ferrari, G. V., and Inestrosa, N. C. (2000) *Brain Res. Brain Res. Rev.* **33,** 1–12
38. Kaytor, M. D., and Orr, H. T. (2000) *Curr. Opin. Neurobiol.* **12,** 275–278
39. Versteeg, R., Caron, H., Cheng, N. C., van der Drift, P., Slater, R., Westerveld, A., Voute, P. A., Delattre, O., Laureys, G., van Roy, N., and Speleman, F. (1995) *Eur. J. Cancer* **31,** 538–541
40. Murata, S., Minami, Y., Minami, M., Chiba, T., and Tanaka, K. (2001) *EMBO Rep.* **2,** 1133–1138
41. Okado-Matsumoto, A., and Fridovich, I. (2002) *Proc. Natl. Acad. Sci. U. S. A.* **99,** 9010–9014
42. Niwa, J., Ishigaki, S., Hishikawa, N., Yamamoto, M., Doyu, M., Murata, S., Tanaka, K., Taniguchi, N., and Sobue, G. (2002) *J. Biol. Chem.* **277,** 36793–36798
43. Mori, K. (2000) *Cell* **101,** 451–454
44. Travers, K. J., Patil, C. K., Wodicka, L., Lockhart, D. J., Weissman, J. S., and Walter, P. (2000) *Cell* **101,** 249–258
45. Wickner, S., Maurizi, M. R., and Gottesman, S. (1999) *Science* **286,** 1888–1893
46. Borchelt, D. R., Lee, M. K., Slunt, H. S., Guarnieri, M., Xu, Z. S., Wong, P. C., Brown, R. H., Jr., Price, D. L., Sisodia, S. S., and Cleveland, D. W. (1994) *Proc. Natl. Acad. Sci. U. S. A.* **16,** 8292–8296

Acta Neuropathol (2004) 107 : 149–158
DOI 10.1007/s00401-003-0791-1

REGULAR PAPER

Shinsuke Kato · Yusuke Saeki · Masashi Aoki · Makiko Nagai · Aya Ishigaki · Yasuto Itoyama · Masako Kato
Kohtaro Asayama · Akira Awaya · Asao Hirano · Eisaku Ohama

Histological evidence of redox system breakdown caused by superoxide dismutase 1 (SOD1) aggregation is common to SOD1-mutated motor neurons in humans and animal models

Received: 8 July 2003 / Revised: 10 October 2003 / Accepted: 13 October 2003 / Published online: 27 November 2003

Abstract Living cells produce reactive oxygen species (ROSs). To protect themselves from these ROSs, the cells have developed both an antioxidant system containing superoxide dismutase 1 (SOD1) and a redox system including peroxiredoxin2 (Prx2, thioredoxin peroxidase) and glutathione peroxidase1 (GPx1): SOD1 converts superoxide radicals into hydrogen peroxide (H_2O_2), and H_2O_2 is then converted into harmless water (H_2O) and oxygen (O_2) by Prx2 and GPx1 that directly regulate the redox system. To clarify the biological significance of the interaction of the redox system (Prx2/GPx1) with SOD1 in SOD1-mutated motor neurons in vivo, we produced an affinity-purified rabbit antibody against Prx2 and investigated the immunohistochemical localization of Prx2 and GPx1 in neuronal Lewy body-like hyaline inclusions (LBHIs) in the spinal cords of familial amyotrophic lateral sclerosis (FALS) patients with a two-base pair deletion at codon 126 and an Ala→Val substitution at codon 4 in the SOD1 gene, as well as in transgenic rats expressing human SOD1 with H46R and G93A mutations. The LBHIs in motor neurons from the SOD1-mutated FALS patients and transgenic rats showed identical immunoreactivities for Prx2 and GPx1: the reaction product deposits with the antibodies against Prx2 and GPx1 were localized in the LBHIs. In addition, the localizations of the immunoreactivities for SOD1 and Prx2/GPx1 were similar in the inclusions: the co-aggregation of Prx2/GPx1 with SOD1 in neuronal LBHIs in mutant SOD1-related FALS patients and transgenic rats was evident. Based on the fact that Prx2/GPx1 directly regulates the redox system, such co-aggregation of Prx2/GPx1 with SOD1 in neuronal LBHIs may lead to the breakdown of the redox system itself, thereby amplifying the mutant SOD1-mediated toxicity in mutant SOD1-linked FALS patients and transgenic rats expressing human mutant SOD1.

Keywords Peroxiredoxin 2 · Glutathione peroxidase 1 · Redox system · Superoxide dismutase 1 · Familial amyotrophic lateral sclerosis

S. Kato (✉) · Y. Saeki · E. Ohama
Department of Neuropathology,
Institute of Neurological Sciences, Faculty of Medicine,
Tottori University,
Nishi-cho 36-1, 683-8504 Yonago, Japan
Tel.: +81-859-348034, Fax: +81-859-348289,
e-mail: kato@grape.med.tottori-u.ac.jp

M. Aoki · M. Nagai · A. Ishigaki · Y. Itoyama
Department of Neuroscience, Division of Neurology,
Tohoku University Graduate School of Medicine, Sendai, Japan

M. Kato
Division of Pathology, Tottori University Hospital,
Yonago, Japan

K. Asayama
Department of Pediatrics,
University of Occupational and Environmental Health,
Kitakyushu, Japan

A. Awaya
Japan Science and Technology Corporation,
Tachikawa, Japan

A. Hirano
Division of Neuropathology,
Department of Pathology, Montefiore Medical Center,
Bronx, New York, USA

Introduction

Living cells produce reactive oxygen species (ROSs) during physiological processes and in response to external stimuli such as ultraviolet radiation. To protect itself from potentially destructive ROSs, each cell of living organisms has developed a sophisticated antioxidant enzyme defense system. In this system, there are two groups of enzymes: the enzymes of the first group convert superoxide radicals into hydrogen peroxide (H_2O_2), and the enzymes of the second group convert H_2O_2 into harmless water (H_2O) and oxygen (O_2). For the first antioxidant enzyme group, three isoforms of superoxide dismutase (SOD) [EC 1.15.1.1] have been identified: SOD1, SOD2, and SOD3 [9]. In the second enzyme group, the peroxiredoxin (Prx) and glutathione peroxidase (GPx) families, as well as catalase localized within peroxisomes have been identified. Unlike

SOD and catalase, enzymes of the Prx and GPx families require secondary enzymes and cofactors to function at high efficiency. In particular, the enzymes of the Prx- and GPx-families are considered to play a role in directly controlling the redox system. In general, the redox system regulates versatile control mechanisms in signal transduction and gene expression [29]. In mammalian cells, this redox signal transduction is linked to systems such as cellular differentiation, immune response, growth control, and apoptosis [10].

Peroxiredoxin2 (Prx2) is a novel organ-specific antioxidative enzyme that is mainly expressed in mammalian brain [23]. This protein is a member of Prx family, whose members possess reactive cysteine residues [23]. Prx2 requires thioredoxin reductase (TR) as a secondary enzyme as well as thioredoxin and NADPH as cofactors to function at high efficiency; the activity of Prx2 in the thioredoxin/TR/NADPH system is over five times higher than that of Prx2 by itself [5]. In this milieu, Prx2 is also called thioredoxin peroxidase 1 (thioredoxin-dependent peroxide reductase 1) or thiol-specific antioxidant [4, 5, 6]. In addition to controlling the intracellular content of H_2O_2, Prx2 directly regulates the redox signals of the thioredoxin/TR/NADPH system, because alone the secondary enzyme and cofactors (i.e., thioredoxin/TR/NADPH) can not directly regulate the redox system and can not act on H_2O_2. Cytosolic GPx [EC 1.11.1.9], a classical selenium-dependent isoform (also assigned as GPx1), was first described as an enzyme that protects hemoglobin from oxidative degradation in red blood cells [25]. The GPx family is composed of at least four GPx isoforms in mammals [7]. Among them, GPx1 is considered as the major enzyme responsible for removing intracytoplasmic H_2O_2. Like Prx2, GPx1 needs glutathione reductase (GR) as a secondary enzyme as well as glutathione and NADPH as cofactors to work at high efficiency, and this process is also one of the redox signals in living cells [21, 24]. Therefore, Prx2 and GPx1 directly control the redox system.

Approximately 20% of the cases of familial amyotrophic lateral sclerosis (FALS) are caused by a mutant SOD1 [15, 17, 18]. SOD1 is thought to be an essential component of neuronal Lewy body-like hyaline inclusions (LBHIs): neuronal LBHIs in affected anterior horn cells are morphological hallmarks of SOD1-mutated motor neurons of FALS patients [3, 11, 12, 13, 14, 15, 16, 17, 18, 30]. To cope with destructive ROSs, even SOD1-mutated motor neurons induce mutant and wild-type SOD1 as well as Prx2 and GPx1. Considering that Prx2 and GPx1 interact not only with wild-type SOD1 but also with mutant SOD1, the interaction of Prx2/GPx1 with SOD1 has been suggested to contribute to mutant SOD1 aggregation toxicity: Prx2/GPx1 possibly aggregate as LBHIs in SOD1-mutated motor neurons. Furthermore, the aggregation of Prx2/GPx1 might affect the intracytoplasmic redox regulation and amplify mutant SOD1-mediated toxicity. To clarify the biological significance of the interaction of Prx2/GPx1 (redox system) with SOD1 in SOD1-mutated motor neurons in vivo, we first produced an antibody against Prx2, and analyzed the characteristic expressions of both Prx2 and GPx1 in neuronal LBHIs in SOD1-mutated motor neurons of humans and animal models.

Materials and methods

Preparation of polyclonal antibody against Prx2

A synthetic peptide corresponding to the C-terminal region of Prx2 (amino acids 184–198: NH_2-KPNVDDSKEYFSKHN-COOH) with or without conjugation to human serum albumin (HSA) at the carboxyl end was supplied by Peptide Institute (Osaka, Japan). This amino acid sequence is homologous with those of the C-terminal region of the human, rat or mouse Prx2. The polyclonal antibody preparation was carried out according to the method of Kato et al. [16]. To prepare immunogen, 6 mg synthesized Prx2 peptide was conjugated with 6 mg keyhole limpet hemocyanin (KLH) in the presence of 50 mM 1-ethyl-3-(3-dimethylaminopropyl) carbodiimide-HCl (Pierce Chemical Co., Rockford, IL) and 2.5 mM *N*-hydroxysulfosuccinimide (Pierce) in 3 ml phosphate-buffered saline (PBS) pH 7.4 for 1 h at room temperature. The reaction was terminated by adding 2-mercaptoethanol to the concentration of 20 mM and dialyzed against PBS for 24 h. To raise polyclonal antibodies, 500 µg of the immunogen in 50% Freund's complete adjuvant was inoculated intradermally into a rabbit at 20 skin sites; four booster inoculations of 500 µg immunogen in 50% Freund's incomplete adjuvant were given at 10, 17, 24 and 31 days after the first inoculation. The serum was taken 10 days after the final immunization. The IgG fraction in the antiserum against the immunogen, the hapten-conjugated KLH, was purified by absorption on a protein G-Sepharose gel column (Pharmacia Biotech, Uppsala, Sweden). Subsequently, the antibodies were further purified on an affinity column of immobilized KLH conjugated with the synthetic Prx2 peptide, as described previously [16].

Enzyme-linked immunosorbent assay

Noncompetitive ELISA was carried out according to the method described by Kato et al. [16]. Each well of a 96-well microtiter plate was coated with 100 µl of 5 µg/ml immunogen in 5 mM sodium carbonate buffer (pH 9.6) and incubated for 60 min. This was followed by triplicate washing with PBS containing 0.05% Tween 20 (buffer A). Each well was blocked with 0.5% gelatin for 60 min and then washed three times with buffer A. Antibody solutions (100 µl) at the concentrations indicated in Fig. 1 (horizontal line) were added to each well and incubated for 60 min. The wells were then washed three times with buffer A. The binding of the horseradish peroxidase-conjugated secondary antibody (Wako Pure Chemical Industries, Osaka, Japan) to the primary antibody was visualized with 2, 2'-azino-bis-(3-ethylbenzothiazoline-6-sulfonate)-$(NH_3)_2$. The reaction was terminated with 1 M sulfuric acid, and the absorbance at 415 nm was read on a micro-ELISA plate reader (Tecan, Hombrechtikon, Switzerland).

Tissue collection

Histochemical and immunohistochemical studies were performed on archival, buffered 10% formalin-fixed, paraffin-embedded tissues obtained at autopsy from five FALS patients who were members of two different families. The main clinicopathological characteristics of the FALS patients are summarized in Table 1, and have been reported previously [12, 13, 20, 22, 28, 30, 31]. SOD1 analysis revealed that the members of the Japanese Oki family had a two-base pair deletion at codon 126 (frame-shift 126 mutation) [12] and the American C family members had an Ala→Val substitution at codon 4 (A4V) [30]. As human controls, we examined autopsy specimens of the spinal cord from 20 neurologically and neuropathologically normal individuals (11 male, 9 females; aged 37–75 years).